

JOINT CONFERENCES
ON ADVANCED MATERIALS AND TECHNOLOGIES

The 12th Workshop
on Functional and Nanostructured Materials
FNMA'15

The 6th International Conference
on Physics of Disordered Systems

PDS'15

The 3rd International Symposium
on Art/Science/Technology

MEDEA'15

6–12 September 2015
Zakynthos, Greece



ABSTRACT BOOK

TITLE

Joint Conferences on Advanced Materials and Technologies:

The 12th Workshop on Functional and Nanostructured Materials – FNMA '15

The 6th International Conference on Physics of Disordered Systems – PDS'15

The 3rd International Symposium on Art/Science/Technology – MEDEA'15

6-12 September 2015, Zakynthos, Greece – Abstract Book

EDITORS

Jarosław Rybicki and Andreas Guskos

TYPESETTING USING \TeX

BOP, www.bop.com.pl

TASK PUBLISHING 2015
GDANSK

ISBN 978-83-937979-5-0

FNMA'15 PDS'15 MEDEA'15
Joint Conferences on Advanced Materials and Technologies
THE 12th WORKSHOP ON FUNCTIONAL AND NANOSTRUCTURED MATERIALS
THE 6th INTERNATIONAL CONFERENCE ON PHYSICS OF DISORDERED SYSTEMS
THE 3rd INTERNATIONAL SYMPOSIUM ON ART/SCIENCE/TECHNOLOGY

ORGANIZERS

Institute of Physics, Faculty of Mechanical Engineering and Mechatronic,
West Pomeranian University of Technology, Szczecin, Poland
Department of Solid State Physics, Gdansk University of Technology, Poland
Department of Solid State Physics, Faculty of Physics, University of Athens, Greece
Technological Educational Institute of Ionian Islands, Greece
Ivan Franko National University of Lviv, Ukraine
Faculty of Visual Arts, Academy of Arts in Szczecin, Poland
Institute of Molecular Physics, Polish Academy of Sciences, Poznan, Poland
University of Zielona Gora, Poland
PWSZ im. Prezydenta St. Wojciechowskiego, Kalisz, Poland

IN COOPERATION WITH:
TASK – Academic Computer Centre in Gdansk, Poland
Poznan Supercomputing and Networking Centre, Poland
Intel Corporation Polish Physical Society

HONORARY CHAIRMEN

W. Kiernozycki (Szczecin, Poland)
G. J. Papadopoulos (Athens, Greece)

SCIENTIFIC COMMITTEE

A. Alderson (Bristol, UK) • F. J. Baltá-Calleja (Madrid, Spain) • J. Barnaś (Poznan, Poland) • J. Bernholc (Raleigh, USA) • X. M. Duan (Beijing, China) • J. Felba (Wroclaw, Poland) • J-G. Gasser (Metz, France) • J. Grima (Msida, Malta) • B. Grzybowski (Evanston, USA) • W. G. Hoover (Ruby Valley, USA) • I. Kaban (Dresden, Germany) • A. B. Kolomeisky (Houston, USA) • A. A. Kornyshev (London, UK) • V. Likodimos (Athens, Greece) • C. A. Londos (Athens, Greece) • H. Mizuta (Southampton, UK) • A. Morawski (Szczecin, Poland) • S. Mudry (Lviv, Ukraine) • O. Mykolaychuk (Lviv, Ukraine) • B. Padlyak (Lviv, Ukraine) • V. Radmilovic (Berkeley, USA) • W. Sadowski (Gdansk, Poland) • N. Sarlis (Athens, Greece) • F. Scarpa (Bristol, UK) • K. Schulte (Hamburg, Germany) • T. Tsuibo (Kyoto, Japan) • I. Vakarchuk (Lviv, Ukraine) • P. Varotsos (Athens, Greece) • K. W. Wojciechowski (Poznan, Poland) • P. Yakibchuk (Lviv, Ukraine) • N. I. Zheludev (Southampton, UK)

PROGRAMME COMMITTEE

M. Dudek (Zielona Gora, Poland) • N. Gouskos (Athens, Greece) • R. Gunnella (Camerino, Italy) • W. Kempinski (Poznan, Poland) • S. Kruchinin (Kiev, Ukraine) • B. Maruszewski (Poznan, Poland) • U. Narkiewicz (Szczecin, Poland) • J. Olchowik (Lublin, Poland) • D. Petridis (Athens, Greece) – Co-Chairman • J. Rybicki (Gdansk, Poland) – Co-Chairman • Ch. Trapalis (Athens, Greece) • J. Typek (Szczecin, Poland)

ORGANIZING COMMITTEE

C. Aidinis (Athens, Greece) • A. Guskos (Szczecin, Poland) • N. Gouskos (Athens, Greece) – Chairman • A. Kampioti (Zakinthos, Greece) • A. Koloryshyn (Lviv, Ukraine) • A. Rybicka (Gdansk, Poland) • J. Rybicki (Gdansk, Poland) • I. Shtablavyy (Lviv, Ukraine) • Sz. Winczewski (Gdansk, Poland) • K. W. Wojciechowski (Poznan, Poland) • G. Zolnierkiewicz (Szczecin, Poland)

CONTENTS

FNMA'2015 and PDS'2015 ABSTRACTS

D. Attard, C. Calleja, R. Cauchi and J. N. Grima <i>Negative Poisson's Ratios in JOZ and LTJ</i>	11
B. Bochentyn, J. Karczewski, T. Miruszewski and B. Kusz <i>Te-Ag-Ge-Sb Thermoelectric Material Fabricated by Novel Oxide Precursor Reduction Method</i>	12
B. Bochentyn, A. Warych, N. Szreder and B. Kusz <i>Te-Ag-Ge-Sb Thermoelectric Material Fabricated by Novel Oxide Precursor Reduction Method</i>	14
A. R. Casha, A. Manché, R. Gatt, D. Attard, K. K. Dudek, W. Wolak, M. Gauci and J. N. Grima <i>The Pathophysiology of Apical Lung Disease: a Biomechanical Hypothesis</i>	15
R. Chmielewski and W. Arabczyk <i>XRD Investigations of Carburization Process of Ammonia Synthesis Catalyst</i>	16
A. Diamantopoulou, S. Glenis, V. Likodimos, G. Zolnierkiewicz and N. Guskos <i>Magnetic Properties of Graphene Oxide and Reduced Graphene Oxide</i>	18
K. K. Dudek, D. Attard, R. Caruana-Gauci, K. W. Wojciechowski and J. N. Grima <i>Unimode Metamaterials with Unusual Compressibility Behaviour</i>	19
J. Dziedzic and C.-K. Skylaris <i>Linear-Scaling Hartree-Fock Exchange and Hybrid Exchange-Correlation Functionals with Plane-Wave Basis Set Accuracy</i>	20
J. Dziedzic and C.-K. Skylaris <i>Minimal-parameter Implicit Solvent Model for Large-scale DFT Calculations</i>	22

J. Dziedzic, S. Winczewski and J. Rybicki <i>On-the-fly Reparameterisation of Metallic Potentials – Applications to Alloy Systems</i>	24
J. P. Formosa, R. Cauchi and J. N. Grima <i>Carbon Allotropes Exhibiting Negative Properties</i>	26
D. Gambin, J. N. Grima, J.-P. Brincat, M. V. Wood, K. M. Azzopardi, D. Attard and R. Gatt <i>Auxetic Behaviour in Molecular Crystals</i>	27
D. Gambin, J. N. Grima and R. Gatt <i>A Study of the Mechanical Properties of Danburite</i>	28
J. N. Grima, K. K. Dudek, D. Attard, R. Gatt, R. Caruana-Gauci and K. W. Wojciechowski <i>Negative Thermal Expansion from Unimode Metamaterials with Triangular Building Blocks</i>	29
M. Grinberg <i>Location of Localized Levels of Ln^{3+} and Ln^{2+} in Solid Band Gap, New Results</i>	30
S. Gulkowski and J. V. Munoz Diez <i>Experimental Analysis and Modeling of I–V Curves of Commercial PV Modules for Different Environmental Conditions</i>	31
N. Guskos, D. Petridis, S. Glenis, A. Diamantopoulou, J. Typek, A. Guskos and P. Berczynski <i>Formation of Magnetic Clusters on Composites of γ-Fe_2O_3 Nanoparticles Covered by $Me_3[Fe(CN)_6]_2 \cdot H_2O$ ($Me(II) = Co(II)$ and $Ni(II)$)</i>	32
N. Guskos, G. Zolnierkiewicz, J. Typek, A. Guskos, P. Adamski, D. Moszyński and W. Arabczyk <i>Magnetic Properties of Nanocomposites from Co-Mo-N System Doped with Cr</i>	33
N. Guskos, G. Zolnierkiewicz, M. Pilarska, J. Typek, C. Aidinis and A. Blonska-Tabero <i>EPR High Temperature Study of $M_3Fe_4V_6O_{24}$ ($M(II) = Cu, Zn, Mg$ and Mn) Compounds</i>	34
N. Guskos, G. Zolnierkiewicz, J. Typek, E. Pilawska, S. Glenis, A. Diamantopoulou, A. Guskos, E. Kusiak-Nejman, A. Wanag, J. Kapica-Kozar and A. W. Morawski <i>EPR Study of TiO_2 Modified with Benzene Vapors at Different Temperatures</i>	36

M. Kempinski, J. Jenczyk and M. Sliwinska-Bartkowiak	
<i>Anisotropic Wetting on Nanostructured Al_2O_3 and Gold Surfaces</i>	38
W. Kempinski, D. Markowski and M. Kempinski	
<i>Conducting Properties of Porous Nano-carbons Steered by Localization Effects</i>	39
I. Kondratowicz and K. Źelechowska	
<i>3D Sponge-like Graphene Hydrogels for Enhanced Oil Adsorption</i>	40
I. Kondratowicz, K. Źelechowska and W. Sadowski	
<i>One-Pot Synthesis of Au-Decorated Reduced Graphene Oxide Cryogels for Bioapplications</i>	41
W. Konicki, A. Hełminiak and W. Arabczyk	
<i>Removal of Anionic Dye Acid Red 88 from Aqueous Solution by Carbon-Coated Magnetic Iron Nanoparticles</i>	42
L. Mizzi, D. Attard, R. Gatt, A. A. Pozniak, K. W. Wojciechowski and J. N. Grima	
<i>Translational Disorder in Hexachiral Honeycomb</i>	43
A. W. Morawski, J. Kapica-Kozar, E. Piróg, E. Kusiak-Nejman, A. Wanag, U. Narkiewicz, B. Michalkiewicz and R. J. Wróbel	
<i>Low-Temperature CO_2 Adsorption on Alkali Metal Titanate Nanomaterials</i>	44
S. Mudry, I. Shtablavyi and U. Liudkevych	
<i>Temperature Dependence of Eutectic Melts Structure</i>	46
S. Mudry and I. Shtablavyi	
<i>Structural Aspects of Liquid-Solid Reactions at Formation of Nanocomposite Systems</i>	47
J. W. Narojczyk, P. M. Pigłowski, K. V. Tretiakov and K. W. Wojciechowski	
<i>Elastic Properties of 2D Hard-Core Repulsive Yukawa Polydisperse Crystals</i>	48
B. V. Padlyak, I. I. Kindrat, S. Mahlik, M. Grinberg, B. Kukliński, N. Guskos, G. Zolnierkiewicz, Y. O. Kulyk and S. I. Mudry	
<i>Spectroscopy of Ce-Doped Borate Glasses</i>	49
G. J. Papadopoulos	
<i>Real Time Quantum Tunneling Through a Double Square Barrier</i>	52

S. Paszkiewicz, A. Szymczyk, I. Pawelec, R. Pilawka and Z. Rosłaniec <i>Electrical and Thermal Conductivity of Polymer Hybrid Nanocomposites Based on PTT-b-PTMO Containing Single-Walled Carbon Nanotubes and Graphene Nanoplatelets.....</i>	53
I. Shtablavyi and V. Plechystyi <i>Influence of Carbon Nanotubes on the Structure of Al-Cu Melts</i>	55
A. Szymczyk, G. Zolnierkiewicz, J. Typek, N. Guskos, I. Pawelec, S. Paszkiewicz, Z. Spitalsky and J. Mosnacek <i>Magnetic Properties of PTT-PTMO/Graphene Oxide-Fe_3O_4 Nanocomposite</i>	56
B. Trawiński, K. Źelechowska, D. Majdecka, J. Karczewski, R. Bilewicz and B. Kusz <i>Carbon Nanotube-Forests as Bioelectrodes for Oxygen Reduction</i>	60
M. Triki, S. Jaziri and R. Bennaceur <i>Interdiffusion in Self-Assembled Quantum Dots Under Annealing Process.....</i>	61
J. Typek, M. Bobrowska, G. Zolnierkiewicz, E. Filipek and A. Paczesna <i>Magnetic Study of $Ni_2Fe_xIn_{1-x}VO_6$ Solid Solutions.....</i>	62
J. Typek, M. Bobrowska, G. Zolnierkiewicz, E. Filipek and A. Paczesna <i>Magnetic Study of $Ni_2Fe_{0.5}In_{0.5}VO_6$ Solid Solution.....</i>	66
J. Typek, K. Wardal, G. Zolnierkiewicz, N. Guskos, D. Sibera, U. Narkiewicz and E. Piesowicz <i>Magnetic Studies of $0.9(Fe_2O_3)/0.1(ZnO)$ Nanocomposite: Polymer Matrix Effect</i>	70
K. Źelechowska, P. Golec, J. Karczewska-Golec, J. Karczewski, A. M. Klonkowski and G. Wągrzyn <i>Peptide-Assisted Synthesis of Metal Oxide Nanostructures.....</i>	74
G. Zolnierkiewicz, B. Kolodziej, N. Guskos, J. Typek, C. Aidinis and E. Pilawska <i>Magnetic Studies of Three Organometallic Copper Complexes.....</i>	75

MEDEA'2015 ABSTRACTS

E. Adam <i>The Phenomenon of Variability in Interior Design in Specific Epochs on the Example of Famous Projects</i>	79
---	----

I. Gawłowicz	
<i>The Terms 'Information Society' or 'Digital Society' in the Language of Public International Law</i>	80
J. N. Grima, A. R. Casha and J. Rybicki	
<i>Natural Architectures in Science, Engineering and Medicine</i>	81
A. Guskos	
<i>Game Engines and New Commercial Market Human-Computer Interfaces on the Way to Web3d</i>	82
N. Guskos, A. Guskos and J. Rybicki	
<i>As It Goes to One Dimension – a Conference Joke.....</i>	83
J. Jurek	
<i>Abstract for the article for the MEDEA2015 Symposium "Space of Overlapping Interaction".....</i>	84
I. Kuriata	
<i>Parallel Techno Creation in Audiovisual Art</i>	85
J. Machnicka	
<i>Empathy in Designing as Manifestation of a New Attitude of Contemporary Designers.....</i>	86
K. Radecka	
<i>Commemoration – an Archetype of Future</i>	87
G. Radecki	
<i>A Diary of a Visual Artist – Hommage‘á Roman Opalka</i>	88
A. Rybicka, J. S. Rybicki, J. N. Grima and J. Rybicki	
<i>Self-Similarity in Architecture</i>	89
A. Rybicka, J. S. Rybicki, J. N. Grima and J. Rybicki	
<i>Architecture vs. Mathematics in Ancient Egypt.....</i>	90
<i>Index of authors</i>	91

**FNMA'2015 and PDS'2015
ABSTRACTS**

Negative Poisson's Ratios in JOZ and LTJ

D. Attard¹, C. Calleja², R. Cauchi¹ and J. N. Grima^{1,2}

¹ *Metamaterials Unit, University of Malta
Msida, MSD 2080, Malta*

² *Department of Chemistry, University of Malta
Msida, MSD 2080, Malta*

Materials with a negative Poisson's ratio exhibit the unusual property of getting fatter when stretched and thinner when compressed. This phenomenon has been reported in a number of materials, including silicates, zeolites and aluminophosphates such as NAT [1], THO [1], APD [1,2] and more recently in STJ [3] amongst others. In this study, force-field based simulations are used to predict the Poisson's ratio of the SiO₂ equivalent frameworks of two recently discovered zeolites: JOZ [4] and LTJ [5], using the CVFF[6] and the Burchart [7] force-fields. The simulations performed predict auxeticity in all three major planes of siliceous LTJ and also in the (100) plane of the siliceous JOZ framework, with maximum auxeticity occurring on axis. A study of the deformation mechanism in the (100) plane of siliceous JOZ suggests that auxeticity can be primarily explained in terms of relative rotations of semi-rigid square units occurring concurrently with some deformation of the units themselves.

References

- [1] J. N. Grima, R. Jackson, A. Alderson and K. E. Evans, *Adv. Mater.*, **12** (2000) 1912
- [2] R. Cauchi, M. Zammit, D. Attard, R. Gatt, J. Rybicki, Sz. Winczewski and J. N. Grima, 10th Conference on Functional and Nanostructured Materials, September 2013, Poros, Greece
- [3] M. Siddorn, F.-X. Coudert, K. E. Evans and A. Marmier, *Phys. Chem. Chem. Phys.*, doi: 10.1039/C5CP01168J
- [4] J. A. Armstrong and M. T. Weller, *J. Am. Chem. Soc.*, **132** (2010) 15679
- [5] R. W. Broach and R. M. Kirchner, *Microporous Mesoporous Mat.*, **143**, (2011) 398
- [6] P. Dauber-Osguthorpe, V. A. Roberts, D. J. Osguthorpe, J. Wolff, M. Genest and A. T. Hagler, *Proteins: Structure, Function and Genetics*, **4** (1998) 31
- [7] E. De Vos Burchart, H. Van Bekkum and B. Van de Graaf, *J. Chem. Soc., Faraday Transactions*, **88** (1992) 2761

Te-Ag-Ge-Sb Thermoelectric Material Fabricated by Novel of Oxide Precursor Reduction Method

B. Bochentyn, J. Karczewski, T. Miruszewski and B. Kusz

*Department of Solid State Physics, Gdańsk University of Technology
Narutowicza 11/12, 80-233 Gdańsk, Poland*

The figure of merit, determining the thermoelectric usage, strongly depends on temperature. The most popular thermoelectric materials at near-room temperature are BiTe-based compounds. Recently BiTe and BiSb materials have experienced a great revival due to the unique properties of their surface electron states (topological insulators) [1,2]. Various scientific groups have reported that developing a solid solution of Bi_2Te_3 and isomorphous compounds such as Sb_2Te_3 , PbTe or GeTe [3,4] leads to a controlled increase in the carrier concentration and to a reduction in the lattice thermal conductivity. Thermoelectric properties can be also controlled by suitable structural modifications. In order to reduce the lattice component of thermal conductivity, such modifications as nanostructuring, forming thin films or forming multilayer systems may be performed. However, these modifications also lead to a decrease in the carrier mobility. One of the solutions can be fabrication of a composite material consisting of grains with different size, however, an optimal ratio between fine and coarse grains should be maintained. Basing on literature reports and the authors' experience in the field of glasses, an innovative method of thermoelectric material fabrication was suggested. Starting from oxide powders, melting at high temperature in air, quenching and reducing in hydrogen should lead to the formation of a complex structure. Various products can be obtained depending on the initial composition of reagents. Moreover, the temperature of reduction will influence the final composition and structure of the fabricated sample. The final product should present both structural and thermoelectrical properties sufficient for thermoelectric applications. For example, it seems to be possible to fabricate a layered structure with a controlled composition and thickness of every layer.

The aim of this work is to present a novel method of thermoelectric materials fabrication. Our investigations have shown that, starting from oxide compounds, it is possible to fabricate multi-component materials, which are very promising for thermoelectric applications, such as Bi-Te, Bi-Sb-Te or Te-Ag-Ge-Sb (TAGS) alloys. The stoichiometry and structure of the final product can be controlled by the methods described in this article. The suggested methodology is easy to apply and allows controlling the structure of the material.

Acknowledgements

This work was partially supported by the National Science Center under Grant No. NCN2012/05/B/ST3/02816

References

- [1] Zhang H., Liu C.-X., Qi X.-L., Dai X., Fang Z. and Zhang S.-C. 2005, *Nat. Phys.* **5** 438
- [2] Hsieh D., Qian D., Wray L., Xia Y., Hor Y.S. and Cava R.J. 2008, *Nature* **452** 970
- [3] Snyder G.J., Toberer E.S. 2008, *Nat. Mater.* **7** 105
- [4] Zheng J.-C. 2011, *Front. Phys. China* **3** 12

Te-Ag-Ge-Sb Thermoelectric Material Fabricated by Novel Oxide Precursor Reduction Method

B. Bochentyn, A. Warych, N. Szreder and B. Kusz

*Department of Solid State Physics, Gdańsk University of Technology
Narutowicza 11/12, 80-233 Gdańsk, Poland*

Bismuth-silicate glasses are applied in low-loss fibre optic and IR-transmitting materials or as the active medium of Raman fibre optical amplifiers and oscillators [1]. They are also used in the production of electron multipliers due to their very high secondary emission coefficient and very high surface conductivity after the reduction in hydrogen [2]. It has been reported [3] that annealing in hydrogen reduces Bi^{3+} ions into neutral atoms, which subsequently agglomerate into granules on the surface and inside glass. If the glass contains also the lead oxide, a similar process of ionic lead reduction to neutral atoms takes place in hydrogen [4]. Then, these lead atoms subsequently agglomerate into granules on the lead-silicate glass surface and in its volume. It has been observed that after reduction in hydrogen a thick layer is formed on the surface of oxide glass samples. According to the results of the EDX analysis this layer is depleted with oxygen related to the glass interior. Many homogenously distributed nano-size granules can be found on the surface of this layer. The nanoindentation investigations indicated that reduction in hydrogen prevents the glass softening. Although the Young modulus of the surface layer formed after reduction is comparable to this parameter of a sample calcined in air, it is much smaller than the Young modulus of the glass interior. The aim of this work is to determine the influence of heat treating conditions (in air and in hydrogen) on the Young modulus and the hardness of various oxide glasses, e.g. Bi-Si-O , Bi-Pb-Si-O , Bi-Ge-O etc.

Acknowledgements

This work was partially supported by the National Science Center under Grant No. NCN2012/05/B/ST3/02816

References

- [1] Witkowska A., Rybicki J., Di Cicco A. 2005, *Journal of Alloys and Compounds* **401** 135
- [2] Trzebiatowski K., Witkowska A., Murawski L. 2000, *Mol. Phys. Rep.* **27** 115
- [3] Kusz B., Trzebiatowski K., Gazda M., Murawski L. 2003, *Journal of Non-Crystalline Solids* **328** 137
- [4] Gackowska J., Gazda M., Trzebiatowski K., Kusz B. 2006, *Journal of Non-Crystalline Solids* **352** 4242

The Pathophysiology of Apical Lung Disease: a Biomechanical Hypothesis

A. R. Casha^{1,2}, A. Manché¹, R. Gatt³, D. Attard³, K. K. Dudek⁴,
W. Wolak⁴, M. Gauci⁵ and J. N. Grima³

¹*Department of Cardiothoracic Surgery, Mater Dei Hospital
Malta*

²*Department of Anatomy, Faculty of Medicine, University of Malta
Msida, MSD 2080, Malta*

³*Metamaterials Unit, Faculty of Science, University of Malta
Msida, MSD 2080, Malta*

⁴*Department of Physics and Astronomy, Uniwersytet Zielonogórski
Zielona Góra, Poland*

⁵*Department of Anaesthesia, Mater Dei Hospital
Malta*

A hypothesis regarding the pathogenesis of apical lung disease is presented. This hypothesis suggests that people born with subclinical congenital apical lung bullae and low Body Mass Index (BMI), a combination present in an otherwise normal fifteen per cent of the population, are predisposed to development of apical lung disease during adolescence and young adulthood, especially in males. The proposed mechanism involves pleural stress levels that depend on the shape of the chest wall which itself changes with development, but has the lowest antero-posterior diameter in the lung apices of low BMI, adolescent and young adult males. In computer simulations of lungs, the site of maximal pleural stress was the apex of lungs with a flattened antero-posterior diameter. High lung stress levels promote the formation of bullae that may burst or become super-infected. This hypothesis was tested for validity in disease progression in secondary tuberculosis (TB) and primary spontaneous pneumothorax (PSP). This abstract is the first to suggest a possible biomechanical mechanism for progression of apical lung disease. This hypothesis successfully predicted that the common pathogenesis of acceleration of pre-existing bullae in low BMI subjects resulted in a higher than expected incidence of concurrent disease in TB reactivation and PSP.

XRD Investigations of Carburization Process of Ammonia Synthesis Catalyst

R. Chmielewski and W. Arabczyk

*Institute of Chemical and Environment Engineering
West Pomeranian University of Technology
Pułaskiego 10, 70-322 Szczecin, Poland*

The carburization process of the ammonia synthesis catalyst was investigated by X-ray diffraction (XRD). The observed values concerning the mean crystallite size and the conversion degrees were determined by the Rietveld method. Pre-reduced nanocrystalline iron, containing structural promoters such as calcium (2.8 wt.%), aluminium (3.3 wt.%) and potassium (0.65 wt.%) oxides that are hard to reduce and form bridges between iron nanocrystallites, was used in the process. The mentioned oxides are nonreactive either with iron or with iron carbide and stabilize the nanocrystalline iron structure at temperatures of the investigated process. Every carburization process was preceded by reduction of the pre-reduced nanocrystalline iron in order to remove the passivated layer of iron oxides. The specific surface area of the studied catalyst in the reduced form, determined by a method based on the BET theory, was $12 \text{ m}^2 \text{ g}^{-1}$. The carburization process was carried out in a differential glass tubular reactor with thermogravimetric measurement of mass changes to obtain a different carburization degree (g_C/g_{Fe}). The process was conducted in methane and at a temperature of 650^0 C . It was found that the carburized samples contained nanocrystalline forms of iron (αFe), iron carbide (Fe_3C) and graphite. The dependence content of αFe in Fe_3C on the carbon content is shown in Figure 1. The initial step of observing to 5.56 wt.% C corresponds to the αFe conversion. For values higher than the stoichiometric composition of Fe_3C (6.67 wt.% C) the carbon deposit nucleation process is observed [1]. The process of Fe_3C decomposition to αFe was observed with the samples examined (Figure 1). Graphite can either build 3D structures or cover

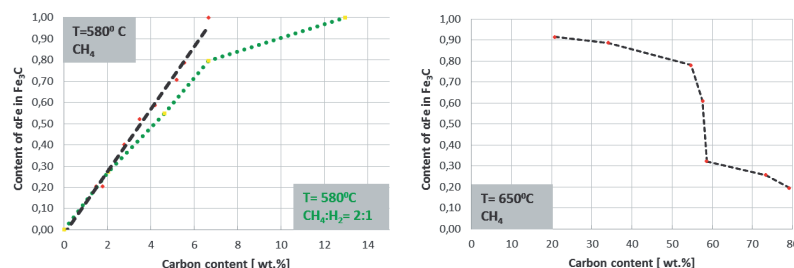


Figure 1: αFe content in Fe_3C in relation to carbon content [1]

the surface of Fe_3C . When the surface of a nanocrystallite of Fe_3C is totally covered by graphite, Fe_3C undergoes decomposition to αFe [2].

References

[1] R. Wrobel, A. Hełminiak, W. Arabczyk, U. Narkiewicz, *J. Phys. Chem. C*, 2014, **118** (28), pp. 15434–15439

Magnetic Properties of Graphene Oxide and Reduced Graphene Oxide

A. Diamantopoulou¹, S. Glenis¹, V. Likodimos¹, G. Zolnierkiewicz²
and N. Guskos²

¹*Department of Solid State Section, Faculty of Physics
University of Athens
Panepistimiopolis, 15 784 Zografou, Athens, Greece*

²*Institute of Physics, West Pomeranian University of Technology Szczecin
Al. Piastów 48, 70-311 Szczecin, Poland*

The evolution of magnetism for graphene oxide (GO) before and after chemical reduction was monitored by means of static magnetization and electron spin resonance (ESR) spectroscopy. The structural properties of pristine GO and chemically reduced graphene oxide (rGO) samples were characterized by Raman and IR-spectroscopy, verifying the efficient reduction of the GO sample. Static magnetization measurements revealed a marked reduction of the strong GO paramagnetism along with an appreciable rise of diamagnetism after chemical reduction, attributed to the drastic removal of paramagnetic defects and the concomitant growth of sp^2 graphitic domains in rGO. This variation was directly corroborated by ESR measurements revealing a large reduction of the spin susceptibility due to paramagnetic defect spins along with the appearance of an asymmetric metallic line shape for the rGO samples. Moreover, the spin susceptibility of both systems was found to be determined by a dominant Curie contribution and a weak temperature independent component ascribed to paramagnetic spin clusters stemming from exchange-coupled localized spins, directly observed over a narrow temperature range (20–40 K) in GO.

Unimode Metamaterials with Unusual Compressibility Behaviour

K. K. Dudek¹, D. Attard¹, R. Caruana-Gauci¹, K. W. Wojciechowski³
and J. N. Grima^{1,2}

¹ *Metamaterials Unit, Faculty of Science, University of Malta
Msida, MSD 2080, Malta*

² *Department of Chemistry, Faculty of Science, University of Malta
Msida, MSD 2080, Malta*

³ *Institute of Physics, Poznan University of Technology
Nieszawska 13A, 60-965 Poznan, Poland*

Rigid unit modes metamaterials based on [Milton, G. W. 2013 *J. Mech. Phys. Solids* **61**, 1543–1560], are analysed by means of the mathematical models for their mechanical properties. It is shown that these unimode systems consisting of rigid scalene triangles exhibit very high positive Poisson's ratios for stretching some directions which can lead to negative linear compressibility along this direction. Such systems expand rather shrink in at least one direction when hydrostatically compressed. It is shown that the actual properties manifested by such systems are dependent on various geometric factors including the actual shape of the units and angle of aperture.

Linear-Scaling Hartree-Fock Exchange and Hybrid Exchange-Correlation Functionals with Plane-Wave Basis Set Accuracy

J. Dziedzic^{1,2} and C.-K. Skylaris¹

¹*School of Chemistry, University of Southampton
Southampton, United Kingdom*

²*Faculty of Applied Physics and Mathematics, Gdańsk University of Technology
Narutowicza 11/12, 80-233 Gdańsk, Poland*

Local and semilocal functionals used in density functional theory (DFT) calculations have long been known to underestimate band gaps and to incorrectly describe the energetics of small molecules, among other deficiencies [1]. The hybrid functional approach, where Hartree-Fock exchange is included into the exchange-correlation functional offers a more accurate description of geometries and of several properties, such as bond energies and band gaps, particularly for metal oxides [2].

We present a resolution-of-identity-based approach [3] for evaluating the Hartree-Fock exchange energy and various hybrid exchange-correlation functionals with a computational cost that scales linearly with the number of atoms. We discuss the conditions that need to be satisfied to ensure the proposed technique is stable and accurate. We describe the implementation of this approach in the linear-scaling DFT code ONETEP [4], which can perform such calculations with near-complete basis set accuracy.

We validate the method against energies, forces and equilibrium bondlengths [2,5] computed with conventional, cubic-scaling DFT codes, demonstrating excellent agreement, even with approaches using an all-electron description and Gaussian basis sets. We show qualitative agreement between B3LYP calculations performed with our technique and the predictions [6] of DFT+U for the binding of O₂ and CO to a simplified model of myoglobin.

We briefly outline how the resolution of identity approach could be used to perform distributed multipole analysis (DMA) of the electronic density.

We conclude with a description of a hybrid (MPI+OpenMP) parallelisation strategy for the proposed implementation, which offers excellent scaling up to hundreds of CPU cores for the calculation of the metric matrix and an outlook on how the remaining sections of the algorithm could be feasibly parallelised. Benchmarks for larger systems, demonstrating the linear-scaling of the computational time with the size of the system will also be presented.

Acknowledgements

J. D. acknowledges the support of the Engineering and Physical Sciences Research Council (EPSRC grant No. EP/J015059/1), of the Ministry of Science and

Higher Education (grant IP2012 043972). C.-K. S. would like to thank the Royal Society for a University Research Fellowship. We would like to thank the University of Southampton for the access to the Iridis4 supercomputer that was used in this work and to the TASK Academic Computer Centre for access to the tryton HPC facility.

References

- [1] M. Marsman, J. Paier, A. Stroppa and G. Kresse, *J. Phys. Cond. Matt.* **20**, 064201 (2008)
- [2] V. N. Staroverov, G. E. Scuseria, J. Tao and J. P. Perdew, *J. Chem. Phys.* **23**, 12129 (2003)
- [3] J. Dziedzic, Q. Hill, C.-K. Skylaris, *J. Chem. Phys.* **139**, 214103 (2013)
- [4] C.-K. Skylaris, P. D. Haynes, A. A. Mostofi and M. C. Payne, *J. Chem. Phys.* **122**, 084119 (2005)
- [5] N. D. M. Hine, M. Robinson, P. D. Haynes, C.-K. Skylaris, M. C. Payne and A. A. Mostofi, *Phys. Rev. B* **83**, 195102 (2011)
- [6] D. J. Cole and D. D. O'Regan and M. C. Payne, *J. Phys. Chem. Lett.* **3**, 1448 (2012)

Minimal-parameter Implicit Solvent Model for Large-scale DFT Calculations

J. Dziedzic^{1,2} and C.-K. Skylaris¹

¹*School of Chemistry, University of Southampton
Highfield, Southampton, UK*

²*Faculty of Applied Physics and Mathematics, Gdańsk University of Technology
Narutowicza 11/12, 80-233 Gdańsk, Poland*

Accurate studies of important biochemical processes, such as protein folding or protein-ligand binding, require that their solvent environment is taken into account in the computation [1]. Explicit inclusion of the solvent with full atomic detail is usually computationally unfeasible, not only because it substantially increases the number of atoms in the system, but also because it necessitates extensive averaging over the solvent degrees of freedom. The implicit solvent (IS) approach introduces an unstructured continuum dielectric to represent the solvent, which seeks to address this difficulty. This averaging property makes IS the prime candidate for use within density functional theory (DFT) calculations on biological systems. Owing to the low directionality and low specificity of most of the solvent's effects, this simplified description is often sufficient to capture the relevant phenomena and provides solvation energies in good agreement with experiment.

A multitude of IS models of differing sophistication have been proposed to date (see [2] for a review). One of the approaches for determining the electrostatic component of solvation involves solving the nonhomogeneous Poisson equation (NPE), or, in saline solutions, a Poisson-Boltzmann equation (PBE), for a system where the solute is placed in a suitably defined cavity, with the dielectric outside of the cavity. The exact shape of the cavity usually depends on a number of parameters. The iso-density formulation of Fettebert and Gygi (FG) [3] instead chooses to define the cavity naturally in terms of the electronic density, which eliminates the need to carefully tune the many cavity parameters present in most other models.

In this work [4,5] we present an implementation of NPE-based solvation models in the ONETEP [6] linear-scaling density functional theory program. ONETEP achieves CPU and memory requirements that increase linearly with the number of atoms by employing a density matrix formulation of DFT using localized functions (Non-orthogonal Generalized Wannier Functions or NGWFs) [7]. We employ the FG formulation and extend it by using consistent open boundary conditions, approximately including dispersion-repulsion interactions and reducing the computational overhead. In so doing, we obtain a fully self-consistent approach, where the electronic density is optimized in the presence of the implicit solvent. Solutions to the NPE are obtained using a high-order defect-corrected multigrid method [8] which we demonstrate is efficient and accurate. We show how the proposed approach consistently gives

predictions in excellent agreement with experiment on a test set of 100+ molecules and demonstrate how it can be used to obtain binding energies in solvent for entire proteins with thousands of atoms, while maintaining good parallel scalability.

Acknowledgements

J. D. acknowledges the support of the Engineering and Physical Sciences Research Council (EPSRC grant No. EP/J015059/1), of the Ministry of Science and Higher Education (grant IP2012 043972) C.-K. S. would like to thank the Royal Society for a University Research Fellowship. We would like to thank the University of Southampton for access to the Iridis4 supercomputer that were used in this work and to the TASK Academic Computer Centre for access to the galera and tryton supercomputing facilities.

References

- [1] N. A. Baker, *Current Opinion in Structural Biology* **15**, 137 (2005)
- [2] J. Tomasi, B. Mennucci and R. Cammi, *Chem. Rev.* **105**, 2999 (2005)
- [3] J.-L. Fattebert and F. Gygi, *Int. J. Quantum Chem.* **93**, 139 (2003)
- [4] J. Dziedzic, H. Helal, C.-K. Skylaris, A. A. Mostofi and M. C. Payne, *Europhys. Lett.* **95**, 43001 (2011)
- [5] J. Dziedzic, S. J. Fox, T. Fox, C. S. Tauterman and C.-K. Skylaris, *Int. J. Quantum Chem.* **113** 771 (2013)
- [6] C.-K. Skylaris, P. D. Haynes, A. A. Mostofi and M. C. Payne, *J. Chem. Phys.* **122**, 084119 (2005)
- [7] C.-K. Skylaris, A. A. Mostofi, P. D. Haynes, O. Dieguez and M. Payne, *Phys. Rev. B* **66**, 035119 (2002)
- [8] S. Schaffer, *Math. of Comp.* **43**, 89–115 (1984)

On-the-fly Reparameterisation of Metallic Potentials – Applications to Alloy Systems

J. Dziedzic^{1,2}, S. Winczewski¹ and J. Rybicki^{1,3}

¹*Faculty of Applied Physics and Mathematics, Gdańsk University of Technology
Narutowicza 11/12, 80-233 Gdańsk, Poland*

²*School of Chemistry, University of Southampton
Highfield, Southampton, UK*

³*TASK Computer Centre, Gdańsk University of Technology
Narutowicza 11/12, 80-233 Gdańsk, Poland*

Molecular dynamics (MD) simulations are an indispensable tool in the study of the mechanical properties of nanoscale systems. The classical nature of MD approaches directly translates to its main limitations, which stem from the empirical nature of the employed potentials, whose functional form is postulated *a priori*, and from not taking the electronic effects explicitly into account. In consequence MD does not correctly model physical reality in all cases, particularly for systems that are far from equilibrium, such as nanostructures undergoing plastic deformation; i.e. classical potentials are said to lack *transferability*.

The explicit inclusion of electronic effects offered by first-principles approaches does yield a transferable description of the interatomic interactions, albeit at a cost of significant computational complexity, usually scaling cubically, or worse, with the system size, which prevents these approaches from being directly applied to systems involving more than several hundred atoms, and even then in practice the performed simulations are usually not dynamical.

Hybrid (quantum-classical) approaches seek a compromise, whereby a subset of the system (such as a region where bond-reorganization is taking place) is treated with a first-principles approach, whilst the remainder undergoes classical MD. The Learn-on-the-Fly (LOTF) technique (Csanyi et al., PRL 93 (17), 2004) offers a particularly elegant way of embedding the results of quantum-mechanical calculations within an MD simulation, by a periodic, local re-parameterisation of the empirical potential so that it reproduces the accurate forces obtained from first principles in the region of interest. In its original formulation it has been successfully applied to the fracture of silicon, where the classical Stillinger-Weber potential is known to give qualitatively wrong predictions.

We present Divide-and-Conquer Learn-on-The-Fly (Dziedzic et al., PRB 83 (22), 2011) – a generalization of LOTF, which is suitable for systems where the interaction range is longer, such as d-shell metals. We show how the force-matching stage can be recast to make the problem of simultaneous optimisation of thousands of parameters *in situ* to match thousands of atomic forces computationally tractable. We demonstrate the feasibility of our approach on several examples: nanoindentation and

nanoscratching of Cu monocrystals, calculation of the structure and properties of liquid metals and the Al-Cu alloy, and the structure of selected AuCu nanoclusters at finite temperature.

Acknowledgements

The authors gratefully acknowledge the funding of the Polish Ministry of Science and Higher Education (grant IP2012 043972).

Carbon Allotropes Exhibiting Negative Properties

J. P. Formosa¹, R. Cauchi² and J. N. Grima^{1,2}

¹*Department of Chemistry, Faculty of Science, University of Malta
Msida, MSD 2080, Malta*

²*Metamaterials Unit, Faculty of Science, University of Malta
Msida, MSD 2080, Malta*

The discovery of new carbon allotropes such as buckyballs, nano-tubes and graphene, has intrigued several chemists and materials scientists to further study new forms of carbon. These systems have the potential to show some unique electrical and thermal properties whilst also exhibiting high strength and hardness. In this study a novel crystalline carbon allotrope, proposed by Hu *et al.* [1] was studied for its potential in exhibiting negative linear compressibility. Through the investigation of the mechanical properties reported in this work [1] as well as through force-field based simulations, it was shown that some of these networks have the potential to exhibit various negative properties. In particular it was shown that the *oC24* and *hP16* networks have the potential in exhibiting negative Poisson's ratio, while the *oC24* was also reported to exhibit negative compressibility. Moreover it was shown that the mechanism and geometries resulting in negative compressibility can be likened to those proposed by Grima *et al.* [2].

References

- [1] Hu Y., Hu M., He J., Wang Q., Huang Q., Yu D., Xu B., *Journal of Superhard Materials*, **36**, 257–269 (2014)
- [2] Grima J. N., Attard D., Caruana-Gauci R., Gatt R., *Scripta Materialia*, **65**, 565–568 (2011)

Auxetic Behaviour in Molecular Crystals

D. Gambin¹, J. N. Grima^{1,2}, J.-P. Brincat¹, M. V. Wood¹,
K. M. Azzopardi¹, D. Attard¹ and R. Gatt¹

¹*Metamaterials Unit, Faculty of Science, University of Malta
Msida MSD 2080, Malta*

²*Department of Chemistry, Faculty of Science, University of Malta
Msida MSD 2080, Malta*

Auxetic materials are materials which exhibit the anomalous behaviour of getting fatter rather than thinner when stretched i.e. they exhibit a negative Poisson's ratio. This anomalous behaviour has been reported in various species, including molecular crystals such as ice, the most common molecular solid present in nature. Studies on ice have attracted the attention of a number of researchers due to its great importance to a number of disciplines including planetary science and geoscience. For instance the presence of ice VII as a stable phase has been reported in portions of the coldest slabs in the oceanic lithosphere.

Though studies on ice have been conducted for over a hundred years, very few studies have focused on the determining the Poisson's ratio of ice. Thus this work has focused on studying the mechanical properties of ice through a number of DFT simulations which work has shown that ice has the potential to exhibit auxetic behaviour. In addition to simulating the structure and mechanical properties of ice our work has also focused on rationalising the predicted negative Poisson's ratio in ice. Our study suggests that the predicted auxetic behaviour in ice could be explained through novel alterations to existing deformation mechanisms.

A Study of the Mechanical Properties of Danburite

D. Gamin¹, J. N. Grima^{1,2} and R. Gatt¹

¹ *Metamaterials Unit, Faculty of Science, University of Malta
Msida MSD 2080, Malta*

² *Department of Chemistry, Faculty of Science, University of Malta
Msida MSD 2080, Malta*

Auxetic materials are materials which exhibit the anomalous behaviour of getting fatter rather than thinner when stretched i.e. they exhibit a negative Poisson's ratio. Several material classes have been studied for their potential to exhibit auxetic behaviour, particularly ceramic materials such as α -cristobalite and β -cristobalite, NAT, THO, EDI and danburite. In view of this, the work carried out in this study aimed to enhance the corpus of knowledge available on ceramic species.

As reported previously, force-field based simulations suggest that the SiO₂ equivalent framework of danburite has the potential to exhibit auxetic behaviour in all the three major planes with maximum auxeticity being exhibited for loading at 45° off-axis. In this work a preliminary investigation on the deformation mechanism of the SiO₂ equivalent framework of danburite was conducted in order to rationalise the suggested negative Poisson's ratio. This preliminary study suggests that the predicted auxetic behaviour is due to a rotating rigid units mechanism where the units involved are not perfectly rigid.

Negative Thermal Expansion from Unimode Metamaterials with Triangular Building Blocks

J. N. Grima^{1,2}, K. K. Dudek¹, D. Attard¹, R. Gatt¹,
R. Caruana-Gauci² and K. W. Wojciechowski³

¹ *Metamaterials Unit, Faculty of Science, University of Malta
Msida, MSD 2080, Malta*

² *Department of Chemistry, Faculty of Science, University of Malta
Msida, MSD 2080, Malta*

³ *Institute of Physics, Poznan University of Technology
Nieszawska 13A, 60-965 Poznan, Poland*

One of the more established mechanisms for generating negative thermal expansion (NTE) is that based on the theory of Rigid Unit Mode (RUM) models. In essence, the concept involves open two dimensional framework structures of particular geometries, composed of rigid units, which experience thermal excitation of low frequency phonon modes (or RUMs) that can experience a shrinkage in the unit cell due to an increased ‘rocking-type motion’ induced by heating. This theory has been found to explain the experimentally measured NTE in a number of classes of materials including β -quartz and tridymite.

The current work will analyse though the RUMs approach a unimode metamaterials with triangular building blocks based on [Milton, G. W. 2013 *J. Mech. Phys. Solids* **61**, 1543–1560] which has pores in the shape of parallelograms. The capability of this system to exhibit negative thermal expansion is confirmed and discussed.

Location of Localized Levels of Ln^{3+} and Ln^{2+} in Solid Band Gap, New Results

M. Grinberg

*Institute of Experimental Physics, University of Gdańsk
Wita Stwosza 57, 80-952 Gdańsk, Poland*

Rare earth ion dopants create luminescence centers in solids that emit due to the internal $4f^n \rightarrow 4f^n$ and $4f^{n-1}5d^1 \rightarrow 4f^n$ transitions. The emission can be excited due to internal absorption (parity allowed $4f^n \rightarrow 4f^{n-1}5d^1$ transition), by band-to-band excitation and nonradiative energy transfer from the excited lattice, by charge transfer transition (CT), and by the ionization process. In the last three cases it is the existence of the intermediate states called impurity trapped exciton (ITE) that is fundamental for an effective excitation lattice-to-impurity energy transfer. In this contribution the spectroscopic investigation of luminescence materials doped with several ions: Ce^{3+} , Pr^{3+} , Tb^{3+} , Dy^{3+} Eu^{3+} and Eu^{2+} is presented. The leading unique experimental technique was high pressure spectroscopy where high hydrostatic pressure is applied in a diamond anvil cell (DAC). High hydrostatic pressure compresses the materials and leads to an increase in the interaction lanthanum ion with the lattice. This changes the energies of localized states related to the $\text{Ln}^{2+(3+)}$ ions and the energies of the band edges. The influence of pressure on luminescence related to the $4f^{n-1}5d^1 \rightarrow 4f^n$ transition in Eu^{2+} and Ce^{3+} and anomalous luminescence related to europium trapped excitation recombination in the case of Eu^{2+} doped fluorides is presented and discussed. The influence of pressure on the ITE states and energy transfer processes in phosphors with Ln^{3+} and Ln^{2+} ions is also analyzed. Specifically the observed pressure induced quenching of the $f - f$ luminescence in Pr^{3+} and Tb^{3+} and pressure induced activation of the luminescence of Eu^{3+} ions is discussed using the model of ITE. It is also discussed how the energies of the ground states of the $\text{Ln}^{2+(3+)}$ with respect to band edges can be determined by the obtained high pressure data.

Experimental Analysis and Modeling of I–V Curves of Commercial PV Modules for Different Environmental Conditions

S. Gulkowski¹ and J. V. Munoz Diez²

¹ *Institute of Renewable Energy Engineering, Lublin University of Technology
Nadbystrzycka 38, 20-618 Lublin, Poland*

² *Grupo de Investigacion IDEA. Escuela Politecnica Superior, Universidad de Jaen
Campus de Las Lagunillas, s/n. 23071- Jaen, Spain*

Investigation of the PV module efficiency in different weather conditions plays a crucial role in production of electricity from photovoltaics. The I–V curve is determined to find the module efficiency. The characteristic parameters of the PV module are estimated on the basis of the curve: the open circuit voltage, the short circuit current and the maximum power point. The shape of the I–V curve depends on the module technology and the weather conditions in which the PV module operates. Irradiation and temperature are the main parameters which influence the generated power of the module.

The experimental method of obtaining the I–V curve is described in this paper. The results of measurements of PV modules produced with use of different technologies are shown. Computer modeling was carried out parallel to the experimental investigation. An equivalent circuit of the photovoltaic cell was used to find the parameters of the nonlinear I–V equation including series and parallel resistance. On the basis of the model the computer simulation was carried out for different irradiation levels and module temperature. The simulation results were compared with the experiments.

Formation of Magnetic Clusters on Composites
of γ -Fe₂O₃ Nanoparticles Covered by
Me₃[Fe(CN)₆]₂ · H₂O (Me(II) = Co(II) and Ni(II))

N. Guskos^{1,2}, D. Petridis³, S. Glenis¹, A. Diamantopoulou¹, J. Typek²,
A. Guskos² and P. Berczynski²

¹*Department of Solid State Section, Faculty of Physics, University of Athens
Panepistimiopolis, 15 784 Zografou, Athens, Greece*

²*Institute of Physics, West Pomeranian University of Technology
Al. Piastów 48, 70-311 Szczecin, Poland*

³*NCSR ‘Demokritos’
Aghia Paraskevi Attikis, 15 341 Athens, Greece*

Magnetic properties of two composites of γ -Fe₂O₃ nanoparticles covered by molecular magnet Me₃[Fe(CN)₆]₂ · H₂O (Me(II) = Co(II) and Ni(II)) were studied. The temperature dependence of dc magnetization in ZFC and FC modes for different applied magnetic fields and the magnetic field dependence of magnetization at different temperatures were recorded for both γ -Fe₂O₃/Co₃[Fe(CN)₆]₂ and γ -Fe₂O₃/Ni₃[Fe(CN)₆]₂. The ZFC magnetization of γ -Fe₂O₃/Co₃[Fe(CN)₆]₂ exhibited an increase for temperatures up to 350 K at the applied magnetic field of 100 Oe. At 500 Oe the transition temperature was revealed and the ZFC magnetization decreased for temperatures down to 300 K. This transition temperature was distinctively lower for the γ -Fe₂O₃/Ni₃[Fe(CN)₆]₂ sample than for the γ -Fe₂O₃/Co₃[Fe(CN)₆]₂ sample at the same value of the magnetic field. The hysteresis loops of both compounds were recorded and the sample with cobalt exhibited a greater value of coercivity field, remanence and magnetization of saturation. At high temperature regions ($T > 100$ K) strong ferromagnetic interactions were observed in both cases. These interactions were stronger for the nickel sample. In both compounds a cluster state was revealed along with a transition from ferromagnetic to antiferromagnetic interactions between the magnetic clusters.

Magnetic Properties of Nanocomposites from Co-Mo-N System Doped with Cr

N. Guskos¹, G. Zolnierkiewicz¹, J. Typek¹, A. Guskos¹, P. Adamski²,
D. Moszyński² and W. Arabczyk²

¹*Institute of Physics, Faculty of Mechanical Engineering and Mechatronics
West Pomeranian University of Technology
Al. Piastów 48, 70-311 Szczecin, Poland*

²*Institute of Chemical and Environment Engineering
Faculty of Chemical Technology and Engineering
West Pomeranian University of Technology
Pulaskiego 10, 70-322 Szczecin, Poland*

Four nanocomposites of mixed phases $n\text{Co}_2\text{Mo}_3\text{N}/(1-n)\text{Co}_3\text{Mo}_3\text{N}$ doped with chromium were prepared. The weight fraction of $\text{Co}_2\text{Mo}_3\text{N}$ phase varied from 7.4%wt. for a sample containing 1%wt. of chromium down to 3.9%wt. of $\text{Co}_3\text{Mo}_3\text{N}$ for a sample containing 2%wt. of chromium. The magnetic dc susceptibility at different temperatures and in different applied magnetic fields in ZFC and FC modes was investigated. Magnetization at low and high temperatures as function of positive and negative magnetic fields was studied. The superparamagnetic state of $\text{Co}_2\text{Mo}_3\text{N}$ nanocrystallites with sizes below 40 nm was detected for two samples. In a high temperature range, $T > 100$ K, the obtained Curie-Weiss temperature was negative for all nanocomposites what suggests the existence of strong antiferromagnetic interactions. Additionally, hysteresis loops were observed at low and high temperatures.

Acknowledgements

This work was supported within the framework of the project financed by the National Centre for Research and Development (*NCBiR*), Agreement PBS2/A1/13/2014.

EPR High Temperature Study of $M_3Fe_4V_6O_{24}$ (M(II) = Cu, Zn, Mg and Mn) Compounds

N. Guskos¹, G. Zolnierkiewicz¹, M. Pilarska¹, J. Typek¹, C. Aidinis²
and A. Blonska-Tabero³

¹*Institute of Physics, West Pomeranian University of Technology
Al. Piastów 48, 70-311 Szczecin, Poland*

²*Department of Electronics-Computers-Telecommunications and Control
Faculty of Physics, University of Athens
Panepistimiopolis, 15 784 Zografou, Athens, Greece*

³*Department of Inorganic and Analytical Chemistry
West Pomeranian University of Technology
Al. Piastów 42, 71-065 Szczecin, Poland*

The crystalline structure and magnetic properties of $M_3Fe_4V_6O_{24}$ (M(II) = Cu, Zn, Mg and Mn) compounds have been presented in Refs. [1–7]. The presence of two magnetic sublattices has been postulated in compounds with non-magnetic metal at the M (II) site. Frustration processes have been detected at low temperatures and magnetic competitive interactions have been identified in the high temperature range (above RT up to 493 K) [6,7]. At room temperature there is a strong and symmetrical line observed in the EPR spectra of all compounds. Figure 1 presents the spectra at different registered temperatures.

The resonance field (H_r) shifted towards higher values with the following temperature gradients: $\Delta H_r/\Delta T=7\times10^{-3}$ mT/K for M(II)=Cu, $\Delta H_r/\Delta T=6\times10^{-3}$ mT/K for M(II)=Zn, $\Delta H_r/\Delta T=6\times10^{-3}$ mT/K for M(II)=Mg, and $\Delta H_r/\Delta T=9\times10^{-3}$ mT/K for M(II)=Mn. The magnetic competition above 220 K changed the direction of resonance line shifts [6]. Samples with nonmagnetic ions displayed almost the same values of the temperature gradient $\Delta H_r/\Delta T$. After introduction of magnetic ions at the M(II) site the gradient increased and its value was significantly larger in manganese compounds because its magnetic moment was much greater than in the copper ion. The temperature dependence of the resonance linewidth showed significant differences in the behavior of compounds containing non-magnetic ions. After an initial decrease with the increasing temperature, at a temperature close to 400 K, it started to increase rapidly which was not observed for the compounds with the magnetic ions at M(II) site. Above 400 K a new phenomenon associated with relaxation processes was observed in which the magnetic system started to freeze and thus obstruct the excess energy transfer. The inverse magnetic susceptibility showed the Curie-Weiss temperature dependence, $\chi(T)=C/(T-T_{CW})$, for all four compounds with the following Curie-Weiss temperatures T_{CW} : 56.4(2), 47.8(2), 17.2(2), and -170.8(2) K for Cu, Zn, Mg, and Mn compounds, respectively. Thus, the strength of interaction was

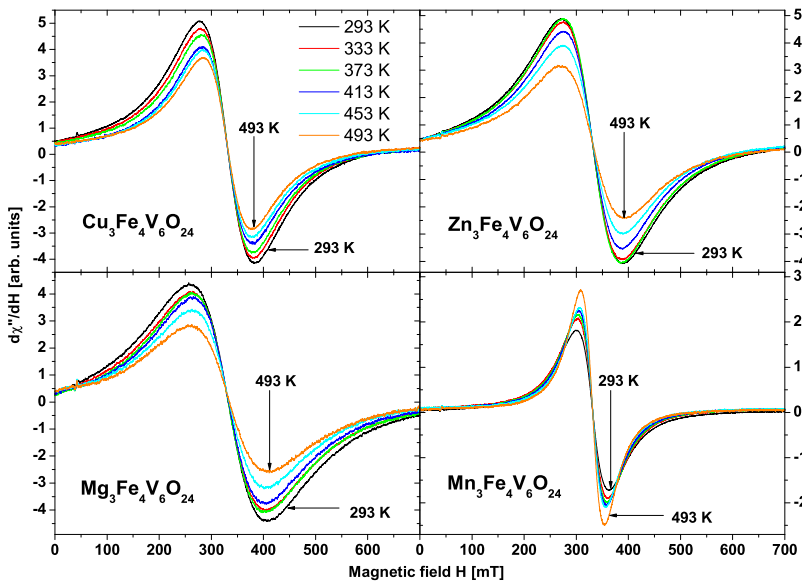


Figure 1: EPR spectra at different temperatures

greater in compounds with magnetic ions than in the Zn and Mg compounds, although the type of interaction may vary (ferromagnetic for copper, antiferromagnetic for manganese).

References

- [1] “Neutron diffraction study of $Mn_3Fe_4V_6O_{24}$ ”, Bezkrovnyi A, Guskos N, Typek J, Ryabova N Yu, Bosacka M, Blonska-Tabero A, Kurzawa M, Rychlowska-Himmel I and Zolnierkiewicz G 2005 *Materials Science-Poland* **23** 883
- [2] “Magnetic resonance study of $M_3Fe_4V_6O_{24}$ ($M=Mg$, Zn, Mn, Cu, Co) compound”, Guskos N, Typek J, Zolnierkiewicz G, Blonska-Tabero A, Kurzawa M and Bosacka M, 2005 *Materials Science-Poland* **23** 923
- [3] “Crystal Structure of $Mg_3Fe_4V_6O_{24}$ Studies by neutron diffraction”, Beskrovnyy A, Guskos N, Typek J, Ryabova N Yu, Blonska-Tabero A, Kurzawa M and Zolnierkiewicz G 2006 *Rev. Adv. Mat. Scie.* **12** 166
- [4] “EPR and TGA study of two $Zn_3Fe_4V_6O_{24-x}$ samples prepared by different thermal treatments”, Zolnierkiewicz G, Guskos N, Typek J and Blonska-Tabero A 2006 *J. Non-Cryst. Solids* **352** 4362
- [5] “EPR Study of magnetic interactions in $Cu_3Fe_4V_6O_{24}$ ”, Zolnierkiewicz G, Guskos N, Typek J and Blonska-Tabero A 2007 *Rev. Adv. Mat. Sci.* **14** 119
- [6] “Competition of magnetic interactions in $M_3Fe_4V_6O_{24}$ ($M(II) = Zn, Cu, Mn, Mg$) compounds studies by EPR at high temperatures”, Zolnierkiewicz G, Guskos N, Typek J, Anagnostakis E A, Blonska-Tabero A and Bosacka M 2009 *J. All. Comp.* **471** 28
- [7] “Magnetic interactions in frustrated $Mn_3Fe_4(VO_4)_6$ ”, Guskos N, Ohta H, Zolnierkiewicz G, Okubo S, Zhang Wei-min, Typek J, Rudowicz C, Szymczak R, Bosacka M, Nakamura T 2009 *J. Non-Cryst. Solids* **355** 1419

EPR Study of TiO_2 Modified with Benzene Vapors at Different Temperatures

N. Guskos¹, G. Zolnierkiewicz¹, J. Typek¹, E. Pilawska¹, S. Glenis², A. Diamantopoulou², A. Guskos¹, E. Kusiak-Nejman³, A. Wanag³, J. Kapica-Kozar³ and A. W. Morawski³

¹*Institute of Physics, West Pomeranian University of Technology
Al. Piastów 48, 70-311 Szczecin, Poland*

²*Department of Solid State Section, Faculty of Physics, University of Athens
Panepistimiopolis, 15 784 Zografou, Athens, Greece*

³*Institute of Inorganic Chemistry and Environment Engineering
West Pomeranian University of Technology
Pułaskiego 10, 70-322 Szczecin, Poland*

Twelve TiO_2 samples subjected to modification with benzene vapours at various calcination temperatures (from 300°C to 850°C, in steps $\Delta t = 50^\circ\text{C}$) were successfully prepared. Electron paramagnetic resonance (EPR) measurements at room temperatures were carried out. EPR spectra were recorded for nine TiO_2 -benzene nanocomposites, consisting of a single resonance line, attributed to free radicals (Fig. 1). No EPR signal was detected for the sample calcined at 550°C, however, EPR spectra arising from magnetic clusters were observed for the sample calcined at 700°C. The linewidth of the registered spectra varied from 0.1 to 0.6 mT. A strong variation of EPR integrated intensities was observed between different samples and the maximum value of this parameter was found for nanocomposite calcinations at 800°C.

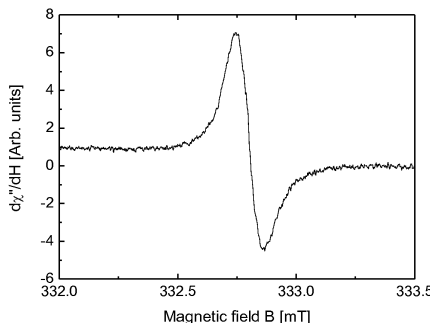


Figure 1: EPR spectrum of TiO_2 nanocomposite modified with benzene vapors at 800°C

The photocatalytic performance of TiO_2 -benzene photocatalysts was conducted on the basis of phenol photodegradation under artificial solar light. The best results were obtained for the photocatalysts calcined at 300 and 350°C with the average

anatase crystallite size of 13 and 14 nm and an average rutile crystallite size of 27 and 30 nm, respectively. A significant change of the composition phase was observed for the photocatalyst calcined in the atmosphere of benzene vapours at 700°C (77% of anatase and 23% of rutile phase).

Acknowledgements

This work was supported under the Maestro 3 No. DEC-2012/06/A/ST5/00226 Project of the National Science Centre (Poland).

Anisotropic Wetting on Nanostructured Al_2O_3 and Gold Surfaces

M. Kempinski^{1,2}, J. Jenczyk^{1,2} and M. Sliwinska-Bartkowiak¹

¹*Faculty of Physics, Adam Mickiewicz University
Umultowska 85, 61-614 Poznan, Poland*

²*NanoBioMedical Centre, Adam Mickiewicz University
Umultowska 85, 61-614 Poznan, Poland*

We present the results of contact angle measurements performed for various liquids on sapphire and gold surfaces with different topographies. Depending on the adhesion/cohesion ratio as well as the surface geometry we observed different behavior of the liquid on a surface and a significant change of the wetting properties. In specific conditions the contact angle depended on the direction of the linear nanostructures present on the surface.

Acknowledgements

We acknowledge the financial support of the National Center of Science, Grants No: DEC-2013/09/B/ST4/03711, DEC-2013/11/B/ST3/04190 and the National Centre for Research and Development under the research grant “Nanomaterials and their application to biomedicine”, Contract No. PBS1/A9/13/2012.

Conducting Properties of Porous Nano-carbons Steered by Localization Effects

W. Kempinski¹, D. Markowski¹ and M. Kempinski²

¹*Institute of Molecular Physics, Polish Academy of Sciences
Smoluchowskiego 17, 60-179 Poznan, Poland*

²*Faculty of Physics and NanoBioMedical Centre, Adam Mickiewicz University
Umultowska 85, 61-614 Poznan, Poland*

Carrier transport through the skeleton of porous carbons depends strongly on the potential barriers which separate elements of the skeleton. According to the hopping mechanism for carriers, percolation paths are created in different graphene-like nano-carbons. Strong spin and charge localization in such materials are observed. These mechanisms will be discussed to explain the specific character of the electrical conductivity behavior in selected nano-carbons.

3D Sponge-like Graphene Hydrogels for Enhanced Oil Adsorption

I. Kondratowicz and K. Żelechowska

*Department of Solid State Physics, Faculty of Applied Physics and Mathematics
Gdansk University of Technology
Narutowicza 11/12, 80-233 Gdańsk, Poland*

Graphene, a two-dimensional layer of graphite, has attracted much attention due to its excellent electrical, mechanical, thermal and optical properties. Efforts have been made to synthesize the three-dimensional graphene structures using graphene oxide (GO) suspension as a precursor [1]. During reduction at higher temperature and elevated pressure (hydrothermal conditions), GO sheets tend to self-assemble into 3D graphene sponge in a form of a hydrogel. The structure shows a high surface area with micro- and macrosize pores, non-uniformly distributed. Sacrificial templates can be used to create the desired architecture of such sponges [2]. We report here the use of silica nanoparticles of different sizes that are captured between GO sheets. After gelation, the silica particles were removed using hydrofluoric acid. As a result, the templated hierarchical nanoporous structures with better-developed outer surface area were obtained. The structure and morphology of non-templated and templated graphene sponges were characterized by X-ray diffraction (XRD), atomic force microscopy (AFM) and scanning electron microscopy (SEM). BET analysis was also performed. The 3D hydrogels exhibited superhydrophobicity, well-developed surface area and good thermal and mechanical stability. Therefore, they show a promising application as adsorbents for removal of oils and organic solvents from wastewater [3]. Moreover, they can be restored by heat treatment to release the adsorbates and thus can be reused again. To investigate the adsorption ability, the materials were immersed in dyed rapeseed oil and observed at intervals of 30 seconds. The oil-uptake capacity for non-templated and templated structures was compared. The latter shows highly efficient adsorption, better than for non-templated graphene hydrogels.

References

- [1] Wu Z. K., Sun Y., Tan Y. Z., Yang S., Feng X. and Mullen K. 2012 *J. Am. Chem. Soc.* **134** 19532
- [2] Sheng H., Dongqing W., Shuang L., Fan Z. and Xinliang F. 2014 *Adv. Mater.* **26** 849
- [3] Chi C. et al. 2015 *Materials Science and Engineering B* **194** 62

One-Pot Synthesis of Au-Decorated Reduced Graphene Oxide Cryogels for Bioapplications

I. Kondratowicz, K. Źelechowska and W. Sadowski

*Department of Solid State Physics, Gdańsk University of Technology
Narutowicza 11/12, 80-233 Gdańsk, Poland*

Graphene – a two-dimensional single layer of carbon atoms – can be obtained through a variety of techniques including physical, chemical and mechanical (e.g. exfoliation) methods. The chemical approach leads to the creation of graphene oxide (GO) – an oxygenated sheet of graphene with hydroxyl, epoxy and carboxyl groups on the edges and the basal plane [1]. The solution-based reduction processes allow removing oxygen-containing functional groups under elevated temperature and pressure. This causes gelation of the GO suspension and production of porous, three-dimensional, sponge-like hydrogels. These reduced graphene oxide structures exhibit a well-developed surface area, good electrical conductivity, chemical inertness and biocompatibility that results in their widespread applications in adsorption of various (bio)molecules. In this work, we demonstrate the facile synthesis of gold nanoparticle (Au)-reduced graphene oxide composites. Graphene-based nanohybrid materials with suspended precious metals have shown to improve the electronic and thermal properties and thus enhance the electrocatalytic activity in fuel and biofuel cells [2]. Graphene sheets were decorated with gold nanoparticles during the simultaneous hydrothermal and chemical reduction of graphene oxide with chloroauric acid (HAuCl_4). The Au-decorated hydrogel was then freeze-dried to obtain cryogel. As a result, the porous structure of cryogel with the spherical gold nanoparticles anchored on a surface and in a bulk was obtained. The morphology of Au-cryogel was studied using scanning electron microscopy (SEM), atomic force microscopy (AFM) and BET analysis. Thermal analysis (TGA) was used to investigate the thermal stability of the nanocomposite. The as-obtained, three dimensional material shows a great promise as a bioelectrode in different biodevices such as biofuel cells or biosensors.

References

- [1] Kondratowicz I, Źelechowska K, Sadowski W 2015 *Optimization of Graphene Oxide Synthesis and Its Reduction* in Nanoplasmonics, Nano-Optics, Nanocomposites, and Surface Studies, O. Fesenko, L. Yatsenko (eds.), Springer Proceedings in Physics 167
- [2] Muszynski R, Seger B, and Kamat P V 2008 *J. Phys. Chem. C* **112** 5263

Removal of Anionic Dye Acid Red 88 from Aqueous Solution by Carbon-Coated Magnetic Iron Nanoparticles

W. Konicki¹, A. Hełminiak² and W. Arabczyk¹

¹*Department of Integrated Transport Technology and Environmental Protection
Maritime University of Szczecin
H. Pobożnego 11, 70-507 Szczecin, Poland*

²*Institute of Chemical and Environment Engineering,
West Pomeranian University of Technology
Pułaskiego 10, 70-322 Szczecin, Poland*

Dyes in water can obstruct light penetration through the water surface and decrease the photosynthetic activity of aquatic organisms. Additionally, some of them have been reported to be carcinogenic and mutagenic for aquatic organisms. Therefore, the removal of textile dyes from water and wastewater is one of the most significant environmental problems. In this study, we investigated adsorption of anionic dye Acid Red 88 from aqueous solution using carbon-coated iron nanoparticles as an adsorbent.

Carbon-coated iron nanoparticles were synthesized by chemical the vapor deposition process using methane as a carbon source and nanocrystalline iron as the catalyst. Before methane decomposition, nanocrystalline iron was reduced polythermally at the temperature raising from 20 to 650°C and next isothermally at 650°C. The synthesis was conducted in a high temperature furnace at 650°C. The prepared adsorbent can be easily separated from the aqueous solution by an external magnetic field.

The adsorption of AR88 was studied in a batch system as a function of pH (3–12), initial AR88 concentration (5–40 mg/L) and temperature (20–60°C). The equilibrium data were analyzed by the Langmuir and Freundlich models of adsorption. The adsorption data fitted well the Langmuir isotherm model. Kinetic analyses were conducted using pseudo first-order, second-order and the intraparticle diffusion models. The results showed that the adsorption kinetics was controlled by a pseudo second-order model for adsorption of AR88 onto CCIN. Additionally, the thermodynamic parameters such as enthalpy ($H\Delta^\circ$), entropy (ΔS°) and Gibbs free energy (ΔG°) were calculated, indicating that the adsorptions of AR88 was spontaneous and exothermic in nature.

Translational Disorder in Hexachiral Honeycomb

L. Mizzi¹, D. Attard¹, R. Gatt¹, A. A. Pozniak²,
K. W. Wojciechowski² and J. N. Grima¹

¹*Metamaterials Unit, Faculty of Science, University of Malta
Msida, MSD 2080, Malta*

²*Institute of Molecular Physics, Polish Academy of Sciences
Smoluchowskiego 17, 60-179 Poznan, Poland*

Chiral honeycombs constitute one of the most important and oft studied classes of auxetic systems due to their vast number of potential applications. Although there have been many studies on these systems, however, very few works have considered the effect of disorder on the mechanical properties of these systems. In view of this, in this study, the effect of translational disorder on hexachiral honeycombs were investigated through a Finite Element approach. It was found that this type of disorder has minimal effect on the Poisson's ratios of these systems provided that the ligament length to thickness ratio remains sufficiently large and the overall length to width ratio of the disordered system does not differ considerably from that of its ordered counterpart. This means that the system is extremely resilient to this type of disorder.

Low-Temperature CO₂ Adsorption on Alkali Metal Titanate Nanomaterials

A. W. Morawski, J. Kapica-Kozar, E. Piróg, E. Kusiak-Nejman,
A. Wanag, U. Narkiewicz, B. Michalkiewicz and R. J. Wróbel

Inorganic Technology and Environment Engineering
West Pomerania University of Technology
Pułaskiego 10, 70-322 Szczecin, Poland

Global warming caused by arising from the emission of greenhouse gases, especially CO₂, has become a most serious issue throughout the world in the recent years. Adsorption with solid sorbents is one of the most promising options to study CO₂ removal from air. Since the work of Kasuga et al. [1], great attention has been paid to hydrothermal synthesis of titanate nanotubes (TNTs) due to the high surface area, uniform pore diameter and unique morphology [2]. This features may suggest potential application as the adsorbent or catalyst support. Recently, extensive research have been conducted on the synthesis, application and characterization of TiO₂ nanotubes (TiNTs). Many research groups have investigated the adsorption of CO₂ on amines such as monoethanolamine (MEA), ethylenediamine (EDA), triethylenetetramine (TETA) and tetraethylenepentamine (TEPA) for nanotube impregnation. Song et al. [3] have investigated the CO₂ adsorption capacity thermal stability of tetraethylenepentamine modified TiO₂ nanotubes and confirmed that the TEPA could be effective materials for CO₂ capture.

The carbon dioxide (CO₂) adsorbents with a high capture efficiency were prepared through a hydrothermal method, then annealed at 350°C in air, and finally

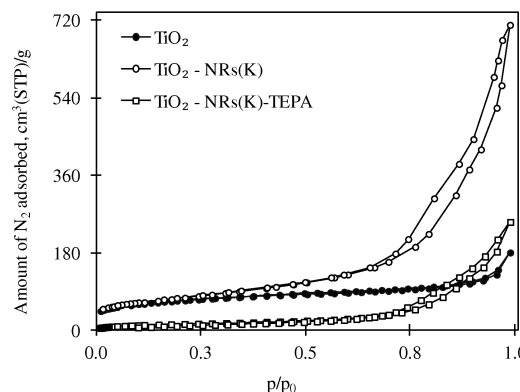


Figure 1: N₂ adsorption/desorption (at 77 K) isotherms

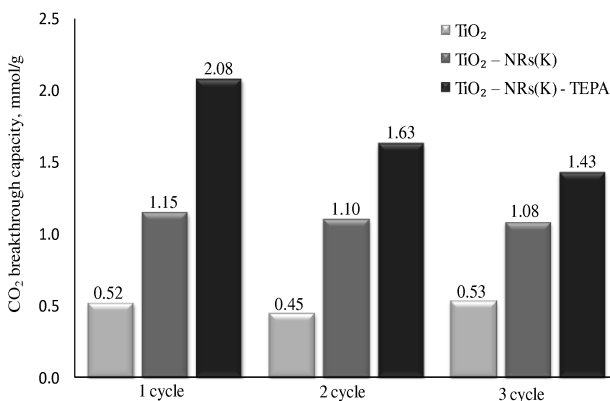


Figure 2: Cycle run of CO_2 adsorption at 30°C and desorption at 100°C

functionalized with tetraethylenepentamine (TEPA). The prepared adsorbents were characterized by N_2 adsorption-desorption at 77 K and X-ray diffraction (XRD). The morphology of the samples was observed with a scanning electron microscope (SEM) equipped with an energy dispersive X-ray spectrometer (EDS) as well as FTIR/DRS and Raman spectroscopy. The CO_2 adsorption performance of the prepared samples was measured using an STA 449 C thermobalance (Netzsch Company, Germany).

Acknowledgements

This work was supported by grant No. Pol-Nor/237761/98/2014

References

- [1] T. Kasuga, M. Hiramatsu, A. Hoson, T. Sekino, K. Niihara, *Adv. Mater.* **11** (1999) 1307
- [2] Q. Chen, G. H. Du, S. Zhang, L. M. Peng, *Acta Crystallogr. B-Struct. Sci.* **58** (2002) 587
- [3] F. Song, Y. Zhao, Q. Zhong, *J. Environ. Sci.* **25** (2013) 554

Temperature Dependence of Eutectic Melts Structure

S. Mudry, I. Shtablavyi and U. Liudkevych

*Department of Physics of Metals, Ivan Franko National University of Lviv
Kyrylo and Mephodii 8, 79005 Lviv, Ukraine*

Most of eutectic alloys reveal an inhomogeneous atomic distribution at temperatures not far from melting point. From numerous structure studies by diffraction methods and measurements of structure-sensitive physical properties it follows that structural units are formed preferentially on the base of like atoms. The main reason for such structure is a significant difference between the atomic radii of constituent atoms and their small electronegativity difference.

With the above in mind we focused our attention on the analysis of temperature dependence of structure parameters in various kinds of eutectic systems: simple eutectics, eutectics with large solubility limits and eutectics with an envelope point in the liquidus curve. The temperature dependencies of structure parameters has been estimated from structure factors and pair correlation functions.

We show that the majority of structure parameters reveal an envelope point in their temperature dependences. We believe this feature to be caused by a transition from a cluster-based structure a structure that resembles a random atomic distribution.

Structural Aspects of Liquid-Solid Reactions at Formation of Nanocomposite Systems

S. Mudry and I. Shtablavyi

*Department of Physics of Metals, Ivan Franko National University of Lviv
Kyrylo and Mephodii 8, 79005 Lviv, Ukraine*

Nanometer-sized materials continue to attract considerable attention in recent years, the primary reason being that the nanometer scale introduces substantial changes to physicochemical properties, relative to the properties of bulk materials. In heterogeneous systems, size effects are influenced also by the morphology of particles, their distribution, and interface interaction. Because of this, investigation of nano-sized heterogeneous systems can play an important role in the understanding of the properties formation process during the manufacturing of materials in the nano-size regime. Metal matrix composites with nanosized metallic or non-metallic fillers are examples of such systems. The synthesis of metal matrix composites filled with metal nanoparticles is confronted with the problem of chemical interaction between the matrix and the metal particles. Such interaction may or may not be beneficial.

For example, chemical interaction of powdered metals and alloys with liquid metals is fundamental to diffusion-hardening solders or the so-called metal glues. In such multicomponent systems, several intermetallic phases form in parallel or in sequence, effecting the phase formation process and the properties of the synthesized material. Literature review indicates that this issue has not yet been addressed in sufficient detail. The formation sequence of intermetallic compounds in systems containing several intermetallics is unclear, and the factors governing this process are as yet not understood. On the other hand, chemical interaction is undesirable in the formation of magnetic fluids with a metal matrix.

For reasons outlined above, the phase formation upon the interaction of fine metal particles with metal matrix have been investigated in this work.

Composites were prepared by mechanical mixing, followed by heat treatment at different temperatures for a variety of durations. Phase analysis was performed based on X-ray powder diffraction data collected with an automatic diffractometer STOE STADI P. The structure in liquid state was investigated by means of high-temperature X-ray diffractometry at a number of temperatures.

Amongst other results, we demonstrate the formation of intermetallic compounds at the solid-liquid boundary.

Elastic Properties of 2D Hard–Core Repulsive Yukawa Polydisperse Crystals

J. W. Narojczyk, P. M. Pigłowski, K. V. Tretiakov
and K. W. Wojciechowski

*Institute of Molecular Physics, Polish Academy of Sciences
Smoluchowskiego 17, 60-179 Poznań, Poland*

The report on studies of mono- and polydisperse crystals in 2D is presented. The investigations are performed using Monte Carlo computer simulations of hard–core repulsive Yukawa particles forming a hexagonal solid phase. The elastic properties of crystalline Yukawa systems are determined in the NpT ensemble with a variable shape of the periodic box. The study concentrates on the influence of the interaction potential properties (Debye screening length κ^{-1} and the potential ϵ) as well as the particle size polydispersity on the elastic properties of the system. Significant influence of the polydispersity on the shear modulus is demonstrated. An increase in the elastic moduli with density is observed, with the growth rate depending on the screening length. A shorter screening length is reflected with a faster increase in the elastic moduli with density and a decrease in the Poisson’s ratio. The studied system is isotropic and exhibits a positive Poisson’s ratio. Thus, in contrast to its three–dimensional version, the system is non–auxetic.

Spectroscopy of Ce-Doped Borate Glasses

B. V. Padlyak^{1,2}, I. I. Kindrat¹, S. Mahlik³, M. Grinberg³,
 B. Kukliński³, N. Guskos⁴, G. Zolnierkiewicz⁴,
 Y. O. Kulyk⁵ and S. I. Mudry⁵

¹ *University of Zielona Góra, Institute of Physics
 Szafrana 4a, 65-516 Zielona Góra, Poland*

² *Vlokh Institute of Physical Optics
 Dragomanov 23, 79-005 Lviv, Ukraine*

³ *University of Gdańsk, Institute of Experimental Physics
 Wita Stwosza 57, 80-952 Gdańsk, Poland*

⁴ *West Pomeranian University of Technology, Institute of Physics
 Al. Piastów 48, 70-311 Szczecin, Poland*

⁵ *Ivan Franko National University of Lviv, Faculty of Physics
 Kyrylo and Mephodii 8, 79005 Lviv, Ukraine*

Spectroscopic properties of Ce-doped crystals and glasses have been an active area of research due to their relatively high light output and fast luminescence decay time. The study of spectroscopic properties of Ce³⁺ ions has also enjoyed fundamental scientific interest as a probe of local crystal field, ion-lattice and ion-ion interactions.

This report presents the results of spectroscopic investigations of a series of Ce-doped borate compounds with different basic compositions as well as the correlation between luminescent properties and the local structure of the Ce³⁺ centres in these compounds using electron paramagnetic resonance (EPR), optical spectroscopy (absorption, photoluminescence, decay kinetics) and X-ray diffraction (XRD) techniques.

Borate compounds doped with Ce₂O₃ in amounts of 0.5 and 1.0 mol.% have been obtained from corresponding melted polycrystals in the air atmosphere using corundum crucibles and standard glass synthesis technology [1]. The obtained Li₂B₄O₇, LiKB₄O₇, and LiCaBO₃ compounds are almost uncoloured and of high optical quality. According to the XRD and EPR data these samples are characterised by a disordered glass structure. Compounds with a CaB₄O₇ composition are characterised by a slightly white colour and are classified as glass-ceramics because their glassy-like XRD pattern contains one sharp peak.

The preliminary results of EPR and optical spectroscopy of Ce-doped borate glasses have been reported in [2]. A broad EPR signal with $g_{\text{eff}} \cong 7.9$ related to the Ce³⁺ isolated centres, a narrow sharp EPR signal with $g_{\text{eff}} \cong 4.26$ of isolated Fe³⁺ non-controlled impurity ions as well as superposition of two broad EPR signals with $g_{\text{eff}} \cong 2.01$ and $g_{\text{eff}} \cong 2.0$ which belong to the Ce³⁺ – Ce³⁺ and Fe³⁺ – Fe³⁺ pair centres, coupled by magnetic dipolar and exchange interactions were clearly observed in all investigated Ce-doped samples at low temperatures (4–20 K) (Figure 1).

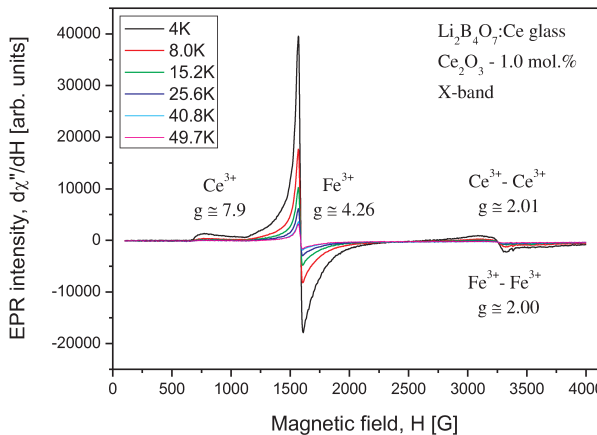


Figure 1: X-band EPR spectra of $\text{Li}_2\text{B}_4\text{O}_7:\text{Ce}$ glass containing 1.0 mol.% Ce_2O_3 , recorded at different temperatures in the 4–50 K range

Optical absorption spectra of the investigated glasses show a weak absorption band picked in the 320–335 nm range ($4f \rightarrow 5d$ transition of the Ce^{3+} ($4f^1$, ${}^2\text{F}_{5/2}$) ions) that overlap with the fundamental absorption edge of the glass host.

The luminescence spectra (emission and excitation) were initially investigated using a FluoroMax-4 (“Horiba”) spectrofluorimeter. More detailed emission spectra and luminescence decay kinetics were registered using special equipment for time-resolved luminescence at the University of Gdansk, described in [3]. In the luminescence spectra the $5d \rightarrow {}^2\text{F}_{5/2}$, ${}^2\text{F}_{7/2}$ emission bands are practically unresolved due to inhomogeneous broadening of the spectral lines that is characteristic for a glassy host. The position of the $5d \rightarrow 4f$ transition strongly depends on the glass composition and varies at the same impurity concentration in the samples from 315 to 340 nm in the excitation bands and from 365 to 415 nm in the emission bands (Figure 2). The observed $5d \rightarrow 4f$ transition of the Ce^{3+} centres in borate compounds is characterised by a large (about 5000 cm^{-1}) Stokes shift. As the Ce concentration in the $\text{Li}_2\text{B}_4\text{O}_7:\text{Ce}$ glass increases, the peaks of the emission and excitation bands slightly shift toward longer wavelengths.

The decay time of the Ce^{3+} emission is very short due to parity and spin-allowed $5d \rightarrow 4f$ transition. The obtained lifetimes lie in the 20 \div 26 ns range and depend on the glass composition and Ce impurity concentration. These dependencies were interpreted in the framework of crystal field splitting of the $5d$ level of Ce^{3+} ions.

The local structure peculiarities of Ce^{3+} centres in the investigated borate compounds have been discussed based on the obtained spectroscopic results, direct EX-AFS (Extended X-ray Absorption Fine Structure) studies [4], and XRD structural data. The X-ray scattering curves were Fourier-transformed to obtain the corresponding pair correlation functions and to derive the average interatomic distances in the glass network. It was shown that the Ce^{3+} centres were localized in the Li (K, Ca) sites of the network of borate compounds (glasses and glass-ceramics), coordinated by O^{2-} positionally-disorder anions. The proposed local structure of the Ce^{3+} centres shows

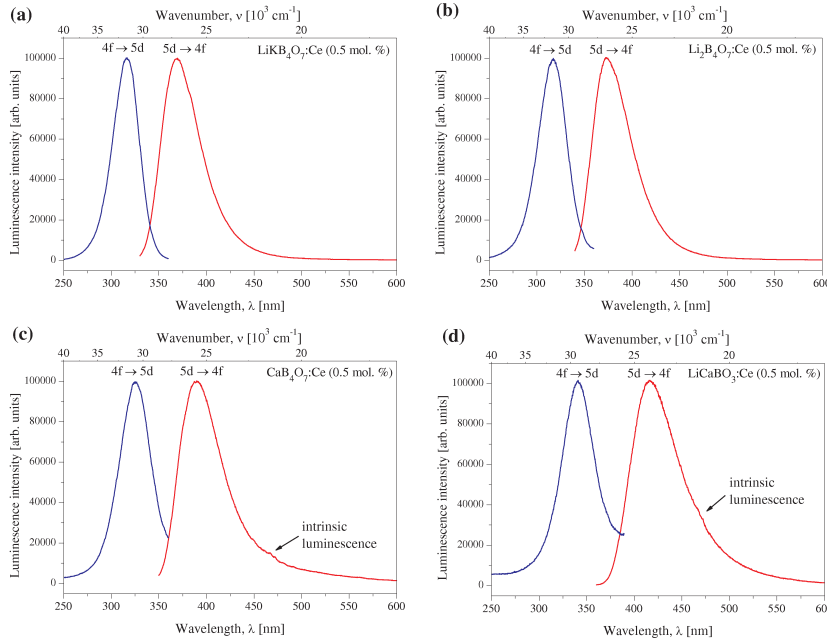


Figure 2: Luminescence excitation and emission spectra of Ce^{3+} centres in the $\text{LiKB}_4\text{O}_7:\text{Ce}$ (a), $\text{Li}_2\text{B}_4\text{O}_7:\text{Ce}$ (b), $\text{CaB}_4\text{O}_7:\text{Ce}$ (c) and $\text{LiCaBO}_3:\text{Ce}$ (d) borate compounds containing 0.5 mol.% Ce_2O_3 at $T = 300\text{K}$

a good correlation with lifetime values and position of luminescence bands. In particular, the observed luminescence band shifts to a longer wavelength with a decrease in the Ce – O average interatomic distance. This effect is related to an increasing crystal field splitting of the $5d$ level and lowering of the lowest crystal-field component from which the emission originates.

The presented results show that the investigated Ce-doped borate glasses and glass-ceramics are promising luminescent materials, especially for effective fast scintillators.

References

- [1] B. V. Padlyak, S. I. Mudry, Y. O. Kulyk, A. Drzewiecki, V. T. Adamiv, Y. V. Burak, I. M. Teslyuk, Synthesis and X-ray structural investigation of undoped borate glasses, *Mater. Sci. Poland* **30** (2012) 264–273
- [2] B. V. Padlyak, I. I. Kindrat, V. O. Protsiuk, B. Kukliński, A. Drzewiecki, V. T. Adamiv, Ya. V. Burak, N. Guskos, G. Żołnierkiewicz, Electron paramagnetic resonance and optical spectroscopy of the Ce-doped borate glasses, *J. Phys. Stud.* **18** (2014) 1998–6
- [3] A. A. Kubicki, P. Bojarski, M. Grinberg, M. Sadownik, B. Kukliński, Time-resolved streak camera system with solid state laser and optical parametric generator in different spectroscopic applications, *Opt. Commun.* **263** (2006) 275–280
- [4] T. D. Kelly, J. C. Petrosky, J. W. McClory, V. T. Adamiv, Ya. V. Burak, B. V. Padlyak, I. M. Teslyuk, N. Lu, L. Wang, W.-N. Mei, P. A. Dowben, Rare earth dopant (Nd, Gd, Dy, and Er) hybridization in lithium tetraborate, *Front. Phys.* **2** (2014) Art 31 1–10

Real Time Quantum Tunneling Through a Double Square Barrier

G. J. Papadopoulos

*Faculty of Physics, Department of Solid State Physics
National and Kapodistrian University of Athens
Panepistimiopolis, 15 784 Zografou, Athens, Greece*

The time evolution of the probability and current densities stemming from an initial state of a particle in the form of a wave packet approaching a double square barrier is studied. This is achieved on the basis of the relevant propagator, via which the corresponding wave function is obtained. There follow numerical results concerning the time evolution of the probability and current densities at the entrance and exit of the barrier, as well as spatial distributions at a given time. Furthermore, the transmission coefficient in terms of the wave packet initial momentum is provided, which shows that transmission is possible even if the momentum, in question, for small values, points away from the barrier. As expected, the transmission coefficient is larger in comparison with the corresponding one in the case of a single barrier with same height and width equal to the sum of the widths of the double barrier.

Electrical and Thermal Conductivity of Polymer Hybrid Nanocomposites Based on PTT-b-PTMO Containing Single-Walled Carbon Nanotubes and Graphene Nanoplatelets

S. Paszkiewicz¹, A. Szymczyk², I. Pawelec², R. Pilawka³
and Z. Rosłaniec¹

¹West Pomeranian University of Technology, Institute of Material Science and Engineering
Al. Piastów 19, 70-310 Szczecin, Poland

²West Pomeranian University of Technology, Institute of Physics
Al. Piastów 19, 70-310 Szczecin, Poland

Nanocomposites based on poly(trimethylene terephthalate-*block*-poly(tetramethylene oxide)) (PTT-PTMO) and hybrid systems of two nanofillers differ in shape, i.e. graphene (3-layer thick, GNP) and single-walled carbon nanotubes (SWCNT) were prepared by *in situ* condensation polymerization following the procedure described previously in [1–4]. A remarkable synergistic effect between the graphene nanoplatelets (GNP) and single-walled carbon nanotubes (SWCNT) in improving the electrical and thermal conductivity of PTT-PTMO based nanocomposites was demonstrated. PTT-PTMO based nanocomposites were prepared with varying combinations of SWCNT and GNP as conducting fillers, and their electrical and thermal conductivity, as well as morphology were evaluated using dielectric spectroscopy, thermal conductivity, SEM, TEM and Raman spectroscopy. It was shown that the addition of SWCNT and GNP enhanced the electrical conductivity of composites: a low percolation threshold was achieved with 0.3 wt.% SWCNT and 0.1 wt.% GNP particles. the schematic mechanism explaining the synergistic effect between SWCNT and GNP in PTT-PTMO based nanocomposites is presented in Fig. 1. However, a remarkable synergistic effect between SWCNT and GNP on improving the electrical conductivity of nanocomposites based on segmented block copolymers was observed. Heterogeneous structure of the PTT-PTMO allowed for a better and more uniform distribution of both types of nanoparticles and stabilized the structure in question. Moreover, in the case of thermal conductivity a synergistic effect was observed for the nanocomposites with 0.5 wt.% of SWCNT and 0.1 wt.% of GNP. The novelty of this work lies in the synergy arising from the combination of two conducting fillers with unique geometric shapes and aspect ratios as well as different dispersion characteristics in the thermoplastic elastomer matrix, which have not been specifically considered previously.

Acknowledgements

The studies were financed by the National Science Centre within the project PRE-LUDE No. 2013/11/N/ST8/00404.

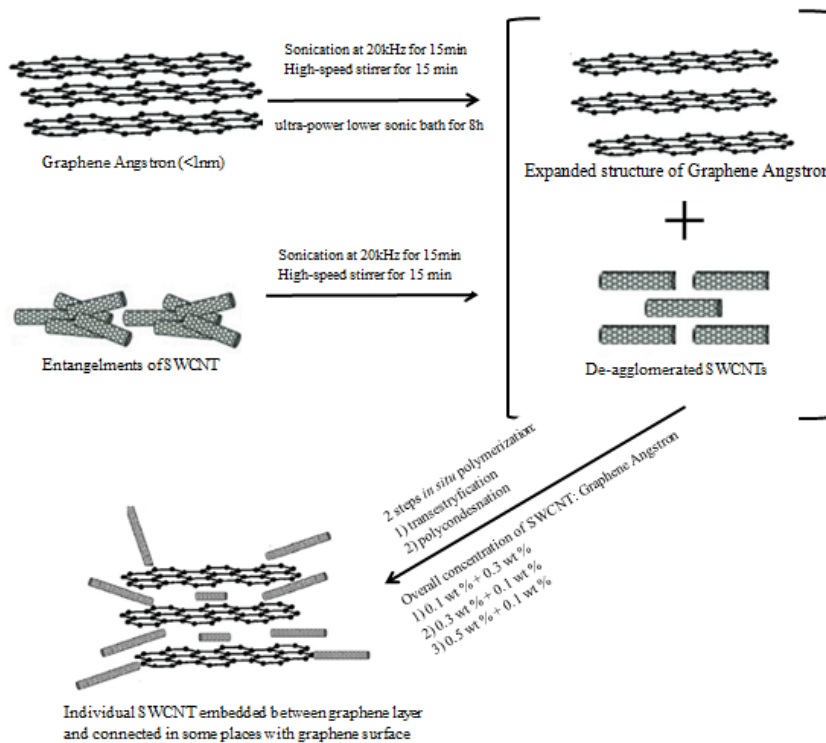


Figure 1: Proposed scheme of mechanism explaining electrical conductivity in PTT-PTMO based nanocomposites

References

- [1] Szymczyk A., Paszkiewicz S., Rosłaniec Z., *Polym Bull* 2013, **70**: 1575–90
- [2] Szymczyk A., Nastalczyk J., Sablong R.J., Rosłaniec Z., *Polym Adv Technol* 2011, **21**, 72–83
- [3] Paszkiewicz S., Szymczyk A., Śpitalski Z., Mosnáček J., Kwiatkowski K., Rosłaniec Z., *Europ Polym J*. 2014, **50**, 69–77
- [4] Paszkiewicz S., Szymczyk A., Livanov K., Wagner H. D., Rosłaniec Z. *eXPRESS Polymer Letters* 2015 (in press)

Influence of Carbon Nanotubes on the Structure of Al-Cu Melts

I. Shtablavyi and V. Plechystyi

*Department of Physics of Metals, Ivan Franko National University of Lviv
Kyrylo and Mephodii 8, 79005 Lviv, Ukraine*

Developing structural materials with satisfactory mechanical properties, particularly simultaneously high values of ductility and strength, is an actual problem of modern materials science. This problem can be addressed by composite materials with a ductile metal matrix with a high-strength filler. Carbon nanotubes are promising fillers for such applications.

In this study the structure of Al-Cu alloys with carbon nanotubes has been investigated. A method for coating carbon nanotubes with metals has been developed, and the results of X-ray diffraction studies of nanotubes coated with copper are presented. Furthermore, the influence of carbon nanotubes on the structure of Al-Cu liquid alloys has been investigated.

Magnetic Properties of PTT-PTMO/Graphene Oxide- Fe_3O_4 Nanocomposite

A. Szymczyk¹, G. Zolnierkiewicz¹, J. Typek¹, N. Guskos¹, I. Pawelec¹,
S. Paszkiewicz², Z. Spitalsky³ and J. Mosnacek³

¹*Institute of Physics, West Pomeranian University of Technology
Al. Piastów 48, 70-311 Szczecin, Poland*

²*Institute of Material Science and Engineering, West Pomeranian University of Technology
Al. Piastów 19, 70-310 Szczecin, Poland*

³*Polymer Institute, Slovak Academy of Sciences
Dubravská cesta 9, 845 41 Bratislavay 45, Slovakia*

In the first step of nanocomposite synthesis graphene oxide (GO) nanosheets, about 5 μm in size, were obtained by using Hummers' method [1], and in the second step graphene oxide was decorated with nano-crystallites Fe_3O_4 , with an average size of 10–20 nm (designated as GO- Fe_3O_4) which were prepared according to the procedure described in [2]. A nanocomposite with 0.5 wt.% of GO- Fe_3O_4 was prepared by *in situ* polymerization [3]. The poly(trimethylene terephthalate)-*block*-poly(tetramethylene oxide) copolymer (designated as PTT-PTMO) was used as the polymer matrix in this nanocomposite. Homogenous dispersion of GO- Fe_3O_4 nanoparticles in the PTT-PTMO matrix was confirmed by the TEM analysis. In Fig. 1 the TEM image of this nanocomposite is shown. It is seen that the PTT-PTMO copolymer formed a continuous phase (grey background) with dispersed GO- Fe_3O_4 nanoparticles (visible as black spots).

The magnetic properties were studied using a SQUID magnetometer in order to investigate the temperature dependence of dc magnetic susceptibility and isothermal magnetization in magnetic fields up to 70 kOe as well as a magnetic resonance spectrometer to examine the ferromagnetic/paramagnetic spectra at a microwave frequency. In Fig. 2 the temperature dependence of magnetic susceptibility in ZFC and FC modes is presented for the GO- Fe_3O_4 nanopowder (a) and this nanopowder dispersed in polymer (b). As is typical for magnetic non interacting nanoparticles the ZFC branch reaches a maximum at the blocking temperature and decreases on sample cooling. A comparison of the ZFC curves in Figs. 2 a) and b) shows that the blocking temperature (~ 200 K) in the nanopowder is significantly increased in comparison to the polymer sample (~ 100 K). It is also the irreversibility temperature (temperature at which the ZFC and FC branches split) is considerably higher in the nanopowder sample. The reason for the increase in both temperatures is strong interaction between nanoparticles (dipole and exchange) due to agglomeration in nanopowder.

In Fig. 3 the isothermal magnetizations of the GO- Fe_3O_4 nanopowder and dispersed in polymer in form of hysteresis loops are shown. The ferromagnetic loops are better developed (higher coercive field and remanence) at low temperature (see

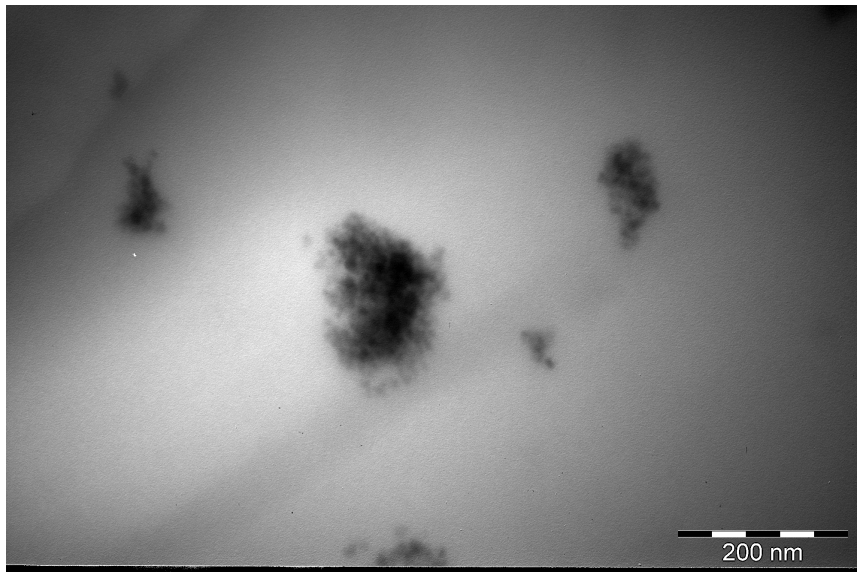


Figure 1: TEM images of PTT-PTMO/0.5GO-Fe₃O₄ nanocomposite, magnification 200 000

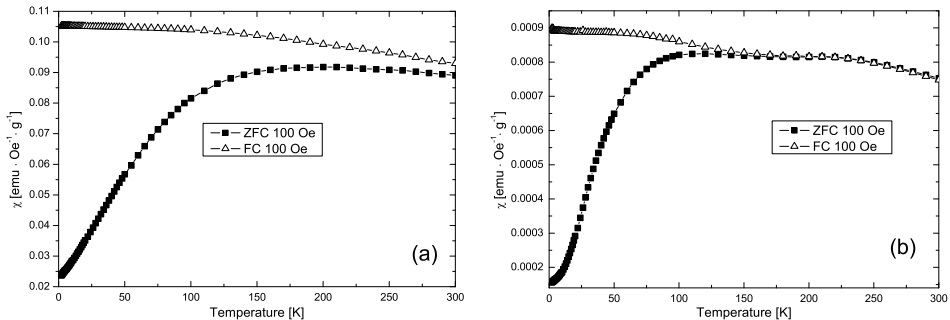


Figure 2: Temperature dependence of dc magnetic susceptibility in ZFC and FC modes for GO-Fe₃O₄ nanopowder (a) and this nanopowder dispersed in polymer (b)

insets). There seems to be no significant superparamagnetic component in magnetization as the M(H) curves saturate at a high magnetic field of several kOe. In polymer samples the diamagnetic contribution of polymer is easily noticed as a decrease in magnetization with the increasing magnetic field. As the sizes of agglomerates are in a relatively broad range, there is some ferromagnetic contribution seen in the M(H) loops even at room temperature.

Figure 4 displays magnetic resonance spectra registered at different temperatures from the 90-300 K range for both studied samples. The spectrum consists of a relatively narrow and asymmetric line that weakens with a temperature decrease. It suggests that the spectrum is produced by a strongly coupled spin system. A comparison of the spectra from the nanopowder and polymer samples shows that the

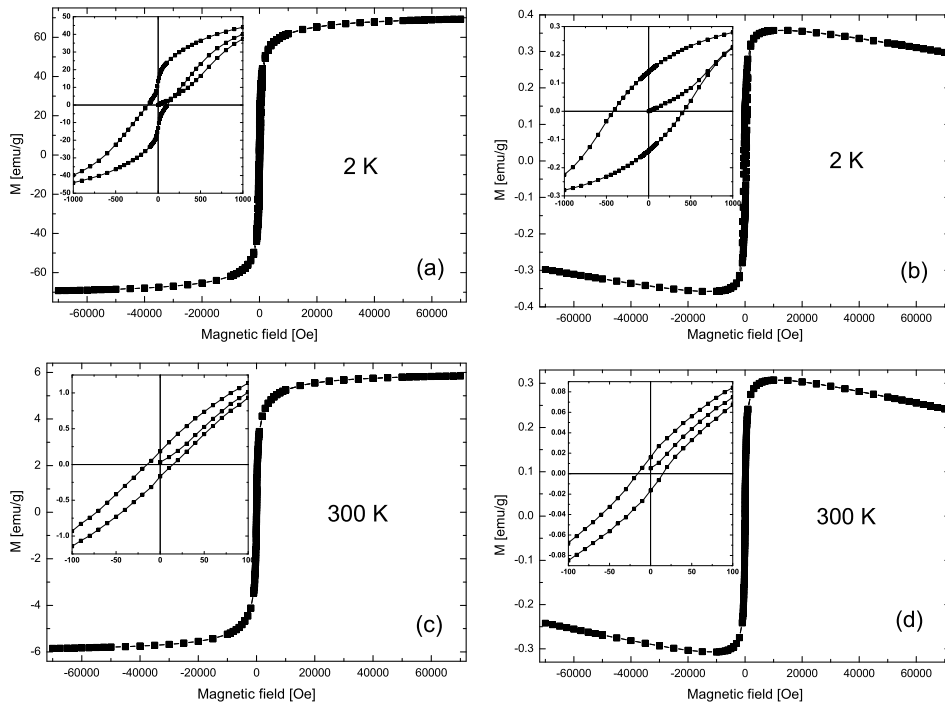


Figure 3: Isothermal magnetization in an external magnetic field at two different temperatures (2 and 300 K) for two samples: nanopowder $\text{GO-Fe}_3\text{O}_4$ ((a) and (c)) and this nanopowder dispersed in polymer ((b) and (d))

resonance line is broader and more asymmetric in the case of the polymer sample. This indicates that the exchange interaction that narrows the line and makes it more symmetric is operating more strongly in the nanopowder sample. It is a reasonable conjecture as large agglomerates of $\text{GO-Fe}_3\text{O}_4$ nanoparticles were detected in that sample.

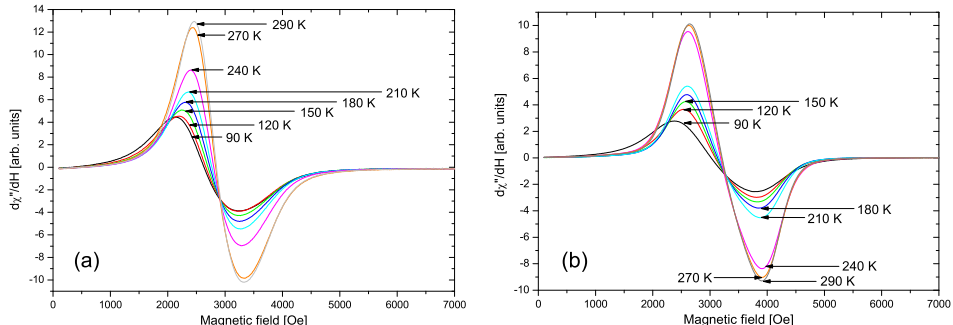


Figure 4: Magnetic resonance spectra registered at different temperatures for nanopowder $\text{GO-Fe}_3\text{O}_4$ (a) and this nanopowder dispersed in polymer (b)

References

- [1] Spitalsky Z, Danko M and Mosnacek J 2011 *Current Organic Chemistry* **vol. 15** pp. 1133-1150
- [2] Wang G, Chen G, Wei Z, Dong X and Qi M 2013 *Materials Chemistry and Physics* **vol. 141** pp. 997-1004
- [3] Paszkiewicz S, Szymczyk A, Spitalsky Z, Mosnacek J, Kwiatkowski K and Rosłaniec Z 2014 *European Polymer Journal* **vol. 50** pp. 69-77

Carbon Nanotube-Forests as Bioelectrodes for Oxygen Reduction

B. Trawiński¹, K. Żelechowska², D. Majdecka³, J. Karczewski²,
R. Bilewicz³ and B. Kusz²

¹ *Student of Faculty of Applied Physics and Mathematics, Gdańsk University of Technology
Narutowicza 11/12, 80-233 Gdańsk, Poland*

² *Department of Solid State Physics, Gdańsk University of Technology
Narutowicza 11/12, 80-233 Gdańsk, Poland*

³ *Faculty of Chemistry, University of Warsaw
Pasteura 1, 02-093 Warsaw, Poland*

Carbon nanotube-forests were synthesized at graphitic substrates with a catalyst using the CVD method. Two different catalysts were used, namely nickel and iron. Graphite rods or carbon papers served as the substrates. The as-obtained nanotube forests were analyzed by SEM imaging with EDX and Raman spectroscopy. The results revealed their multi-walled morphology with diameters c.a. 30-50 nm. The chemical functionalization of nanotube-forests was performed by free radical reaction. Aminonaphthalene was converted into aminonaphthalene diazonium salt, which was next thermally decomposed generating nitrogen and naphtyl radicals reacting with the carbon network. The chemically functionalized nanotube-forests were examined by spectroscopic and electrochemical methods. Chemically functionalized nanotube-forests were tested as electrodes for biocatalytic oxygen reduction by laccase. The obtained current densities reached 200 $\mu\text{A}/\text{cm}^2$ making the presented structure a promising material for bioelectrodes.

References

[1] Karaśkiewicz M., Nazaruk E., Żelechowska K., Biernat J. F., Rogalski J. *Fully enzymatic mediatorless fuel cell with efficient naphthylated carbon nanotube–laccase composite cathodes*, R. Bilewicz. *Electrochemistry Communications* **20** (2012) 124–127

Interdiffusion in Self-Assembled Quantum Dots Under Annealing Process

M. Triki¹, S. Jaziri^{1,2} and R. Bennaceur¹

¹*Laboratoire de Physique de la Matière Condensée, Faculté des Sciences de Tunis
Tunisia*

²*Laboratoire de Physique et des Matériaux, Département de Physique
Bizerte, Tunisia*

Although better performance of optoelectronic devices was expected from self-assembled quantum dots (QDs), it has been found that such a method of growth usually results in ensembles of dots that vary in size and shape, resulting in inhomogeneous broadening of their photoluminescence emission which has a negative effect on their performance and constitutes a technical barrier for the development of QD-based devices. Therefore, the need to use a narrowing technique of the photoluminescence emission of self assembled QDs is a major goal. On the other hand, many experiments have evidenced optical emission narrowing of self-assembled QDs after a rapid annealing process. In fact, high temperatures induce interdiffusion of QD constituents, leading, in addition to spectra shifts, to more uniformity in the shape of dots, and thereby sharper photoluminescence intensity.

The inter-diffusion in InAs/GaAs QDs under an annealing process is investigated in this work. Its influence on the compositional band offsets and effective mass profiles is discussed. The carrier spectra and optical transitions under the an annealing process are calculated.

Magnetic Study of $\text{Ni}_2\text{Fe}_x\text{In}_{1-x}\text{VO}_6$ Solid Solutions

J. Typek¹, M. Bobrowska¹, G. Zolnierkiewicz¹, E. Filipek²
and A. Paczesna²

¹*Institute of Physics, West Pomeranian University of Technology
Al. Piastów 48, 70-311 Szczecin, Poland*

²*Department of Inorganic and Analytical Chemistry
West Pomeranian University of Technology
Al. Piastów 42, 71-065 Szczecin, Poland*

Magnetic studies of $\text{Ni}_2\text{Fe}_x\text{In}_{1-x}\text{VO}_6$ solid solutions ($0 < x < 1$) are presented. The investigated compounds (with $x = 0, 0.1, 0.25, 0.50, 0.75$ and 1.00) are formed in a two-component system which is built by isostructural Ni_2InVO_6 and Ni_2FeVO_6 . It has been also found that this solution is of a substitutional nature, i.e. it is formed by incorporation of Fe^{3+} ions instead of In^{3+} ions in the Ni_2InVO_6 matrix. Monophase samples containing $\text{Ni}_2\text{In}_{1-x}\text{Fe}_x\text{VO}_6$ can be obtained by heating $\text{Ni}_2\text{InVO}_6/\text{Ni}_2\text{FeVO}_6$ mixtures in air as well as by sintering mixtures of oxides V_2O_5 , In_2O_3 , Fe_2O_3 , $2\text{NiCO}_3 \cdot 3\text{Ni(OH)}_2 \cdot 4\text{H}_2\text{O}$ – as a precursor of NiO . The powder samples obtained in such way crystallize in an orthorhombic system and melt in the temperature range from 1330°C (for Ni_2InVO_6) to 1250°C (for Ni_2FeVO_6).

The magnetic structure of the mixed valence Ni_2FeVO_6 – and probably also other studied solid solutions – is very complex. Previous experimental and theoretical magnetic investigations of Ni_2FeVO_6 have revealed that nickel ions are separated from iron and vanadium ions, forming strong antiferromagnetic (AFM) layers with high Neel temperature and thus do not contribute to spontaneous magnetization. Layers containing Fe^{3+} ions may also contain vanadium ions exhibiting three valences (3+, 4+, and 5+ with spins 1, 1/2, and 0, respectively). As the distribution of vanadium ions inside iron layers is random, this makes a really complicated two dimensional case of magnetism. A simplified theory taking in account only the Fe-Fe interactions modified by V ions of three different kinds was put forward. This random-bond Ising model (RBIM) was considered and applied with success to explain the temperature step-wise dependence of magnetization of Ni_2FeVO_6 . The final conclusion is that RBIM gives a qualitatively good explanation of the magnetization under the assumption that there is a small number of strong bonds while all other bonds are much weaker.

The powder samples investigated in this study were obtained by a traditional calcination method. Two investigation methods were used to characterize the solid solution magnetically: dc SQUID magnetometry and electron paramagnetic resonance (EPR). The magnetization studies were carried out on the Quantum Design Magnetic Property Measurements System MPMS XL-7 with a superconducting quantum interference device magnetometer in magnetic fields up to 70 kOe and in the 2–300 K temperature range. The EPR spectra of solid solutions in the powder form were recorded on a conventional X-band Bruker ELEXSYS E 500 spectrometer operating

at 9.5 GHz with the 100 kHz magnetic field modulation. The first derivative of the absorption spectra was been recorded as a function of the applied magnetic field. The temperature dependence of the EPR spectra of the solid solutions under study in the 90-290 K temperature range was recorded using an Oxford Instruments ESP helium-flow cryostat and in the 300-500 K range using a homemade high-temperature attachment.

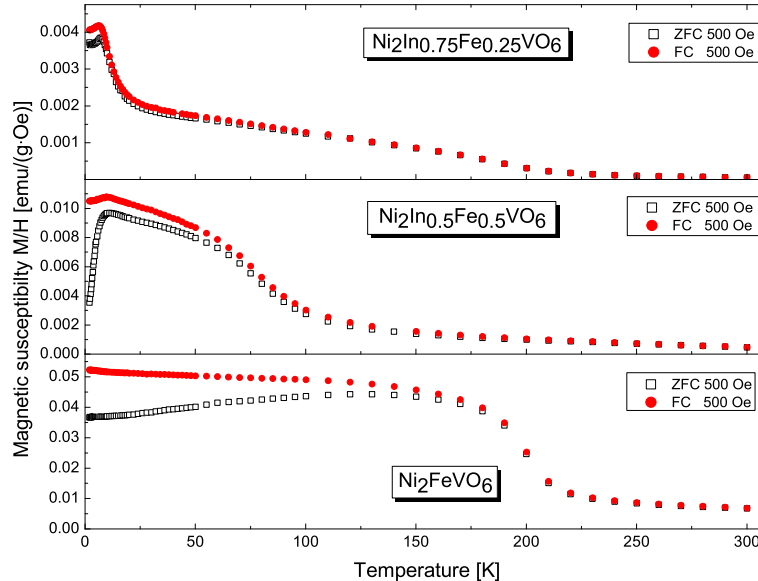


Figure 1: Temperature dependence of dc magnetization M/H in FC and ZFC modes in an external magnetic field $H = 500$ Oe for three different solid solutions

The temperature dependence of magnetic susceptibility (Fig. 1) reveals the presence of several different magnetic components and strong similarity to the nanoparticle magnetic response in the low temperature range. The effect of thermomagnetic irreversibility (branching of ZFC and FC curves at certain temperature) is often observed, e.g. in the case of ferromagnetic compounds and magnetic nanoparticles in the superparamagnetic phase.

The isothermal magnetization study of $\text{Ni}_2\text{Fe}_x\text{In}_{1-x}\text{VO}_6$ solid solutions (Fig. 2) showed that except for sample $x = 1$, no saturation – even in the strongest available field (70 kOe) – was reached, what is typical for paramagnetic, superparamagnetic and antiferromagnetic phases. As we expected to encounter different spin nanoclusters in layers of the $\text{Ni}_2\text{Fe}_x\text{In}_{1-x}\text{VO}_6$ samples we tried to fit the $M(H)$ dependence by the Langevin and modified Langevin functions which were used e.g. in the superparamagnetic phase of magnetic nanoparticles. The best results were achieved using the modified Langevin function, $M = M_S \cdot pL(x) + \alpha H$, where $L(x) = \coth(x) - \frac{1}{x}$ is the Langevin function and $x = \frac{\mu_p H}{kT}$. Here M_S is the saturation magnetization, μ_p is the particle magnetic moment, k is the Boltzmann constant and α is the linear susceptibility. The obtained values of $M_S(0)$ were used to determine the value of the magnetic moment (in Bohr magnetons μ_B) of the $\text{Ni}_2\text{Fe}_x\text{In}_{1-x}\text{VO}_6$ formula unit.

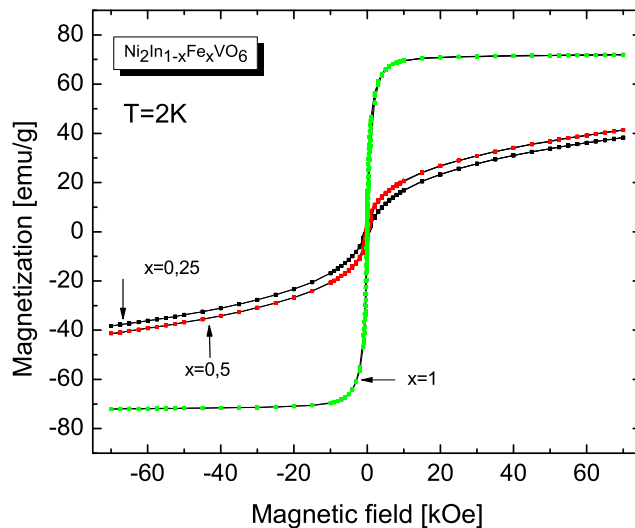


Figure 2: Isothermal magnetization M of three solid solutions at 2 K

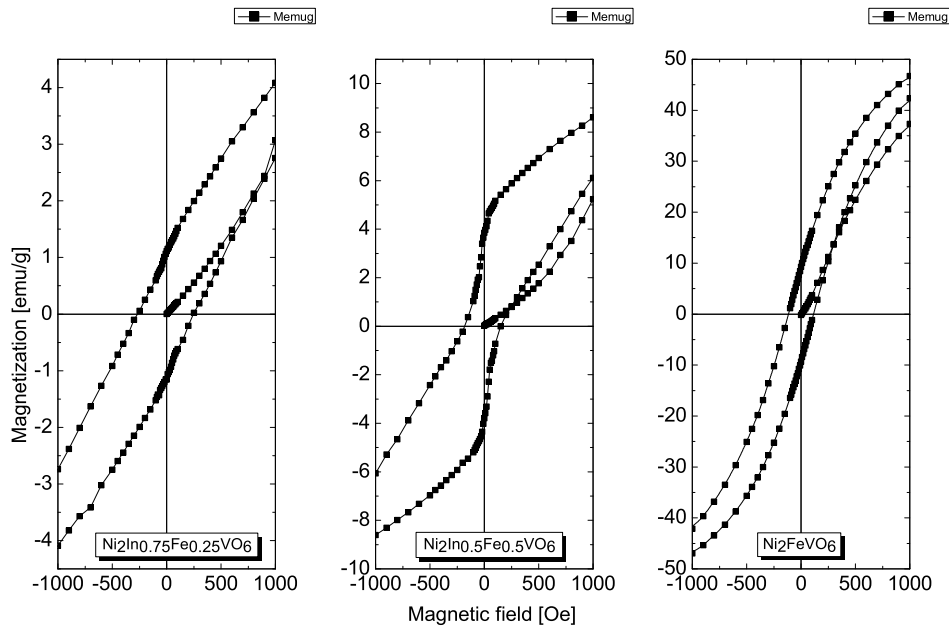


Figure 3: Central part of hysteresis loop registered at 2 K for three different solid solutions

Hysteresis is observed in the magnetization of $\text{Ni}_2\text{Fe}_x\text{In}_{1-x}\text{VO}_6$ solid solutions in weak magnetic fields. Figure 3 shows the central part of hysteresis loops observed for three samples taken at 2 K. The remanent magnetization (remanence) and the

coercive field (coercivity) determined from the loop decrease strongly with increasing temperature. The dependence between these two hysteresis loop parameters is nearly linear.

Strong EPR signals were registered in the 4-300 K range. These signals are typical for a strongly coupled system of iron ions (Fig. 4). The spectra taken at different temperatures were analyzed in terms of component lines and the determined EPR parameters (resonance field, linewidth, integrated intensity) of these components were used to reveal the magnetic complexes responsible for the spectra.

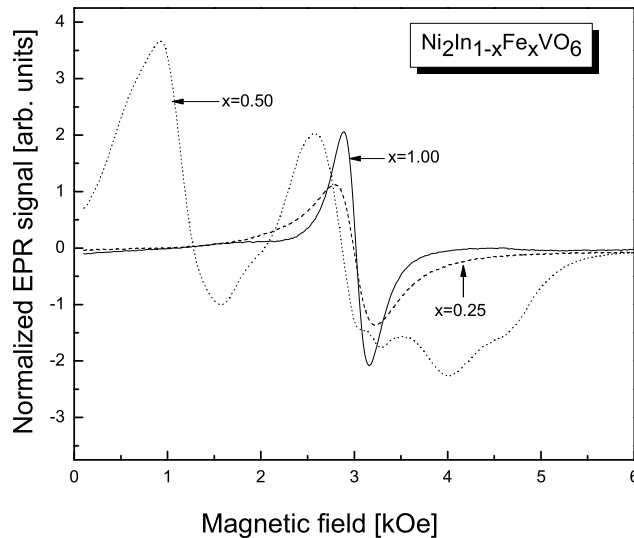


Figure 4: EPR spectra of $\text{Ni}_2\text{Fe}_x\text{In}_{1-x}\text{VO}_6$ solid solutions recorded at room temperature

Both types of magnetic measurements (dc magnetization and magnetic resonance) give a consistent picture of the magnetic structure of the $\text{Ni}_2\text{Fe}_x\text{In}_{1-x}\text{VO}_6$ solid solution. Its magnetic properties are dependent in a large part on Fe^{3+} ions in a high spin state that are located in layers containing also indium and vanadium ions. Different Fe^{3+} complexes involving also magnetic V^{3+} and V^{4+} ions can be found in these iron layers. The magnetization study has revealed at least three different types of magnetic complexes. It is suggested that the sizes of magnetic complexes in $\text{Ni}_2\text{Fe}_x\text{In}_{1-x}\text{VO}_6$ solid solutions might be in the nanometric range.

Magnetic Study of $\text{Ni}_2\text{Fe}_{0.5}\text{In}_{0.5}\text{VO}_6$ Solid Solution

J. Typek¹, M. Bobrowska¹, G. Zolnierkiewicz¹, E. Filipek²
and A. Paczesna²

¹*Institute of Physics, West Pomeranian University of Technology
Al. Piastów 48, 70-311 Szczecin, Poland*

²*Department of Inorganic and Analytical Chemistry
West Pomeranian University of Technology
Al. Piastów 42, 71-065 Szczecin, Poland*

The results of magnetic studies of the $\text{Ni}_2\text{Fe}_{0.5}\text{In}_{0.5}\text{VO}_6$ solid solution are presented. A powder sample of $\text{Ni}_2\text{Fe}_{0.5}\text{In}_{0.5}\text{VO}_6$ that belongs to a two-component system built by the isostructural compounds Ni_2InVO_6 and Ni_2FeVO_6 was obtained by a traditional calcination method. Two investigation methods were used to characterize the solid solution magnetically: dc SQUID magnetometry and electron paramagnetic resonance (EPR). The magnetization measurements revealed a step-like temperature dependence (Fig. 1) demonstrating the presence of a few different types of magnetic entities confined to separate layers of trivalent indium and iron ions as well as possible vanadium ions in different valence states. The magnetism of iron ions forming diverse nanocomplexes plays a central role in the generation of magnetic properties of $\text{Ni}_2\text{Fe}_{0.5}\text{In}_{0.5}\text{VO}_6$.

In Fig. 2 isothermal magnetization of $\text{Ni}_2\text{Fe}_{0.5}\text{In}_{0.5}\text{VO}_6$ registered at six different temperatures is shown. No saturation – even in the strongest available field (70 kOe) – was reached, what is typical for paramagnetic, superparamagnetic and AFM phases. As we expected to encounter different spin nanoclusters in layers of $\text{Ni}_2\text{Fe}_{0.5}\text{In}_{0.5}\text{VO}_6$ we tried to fit the $M(H)$ dependence by the Langevin and modified Langevin functions which were used e.g. in the superparamagnetic phase of magnetic nanoparticles. It was found that the best result for our $\text{Ni}_2\text{Fe}_{0.5}\text{In}_{0.5}\text{VO}_6$ solid solution was achieved using the modified Langevin function, $M = M_S \cdot pL(x) + \alpha H$, where $L(x) = \coth(x) - \frac{1}{x}$ is the Langevin function and $x = \frac{\mu_p H}{kT}$. Here M_S is the saturation magnetization, μ_p is the particle magnetic moment, k is the Boltzmann constant and α is the linear susceptibility.

Hysteresis is observed in the magnetization of $\text{Ni}_2\text{Fe}_{0.5}\text{In}_{0.5}\text{VO}_6$ in weak magnetic fields. Fig. 3 shows the central part of hysteresis loops observed for $\text{Ni}_2\text{Fe}_{0.5}\text{In}_{0.5}\text{VO}_6$ at 2 K (left panel) and 300 K (right panel). It is remarkable that the loop is detected even at room temperature. The remanent magnetization (remanence) and the coercive field (coercivity) determined from the loop decrease strongly with increasing temperature. The dependence between these two hysteresis loop parameters is nearly linear.

The strong EPR signal that was registered in the whole investigated temperature range is typical for a strongly coupled system of iron ions. Selected EPR spectra of $\text{Ni}_2\text{Fe}_{0.5}\text{In}_{0.5}\text{VO}_6$ solid solution recorded at different temperatures are shown in Fig. 4 as an example. A high temperature EPR spectrum composed of several components

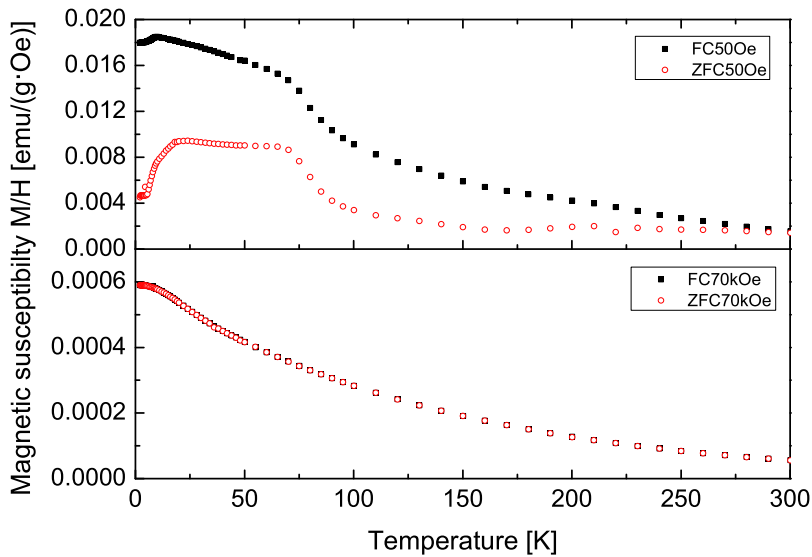


Figure 1: Temperature dependence of magnetic susceptibility M/H in ZFC and FC modes in two external magnetic fields: $H = 50$ Oe (upper panel) and $H = 70$ kOe (lower panel)

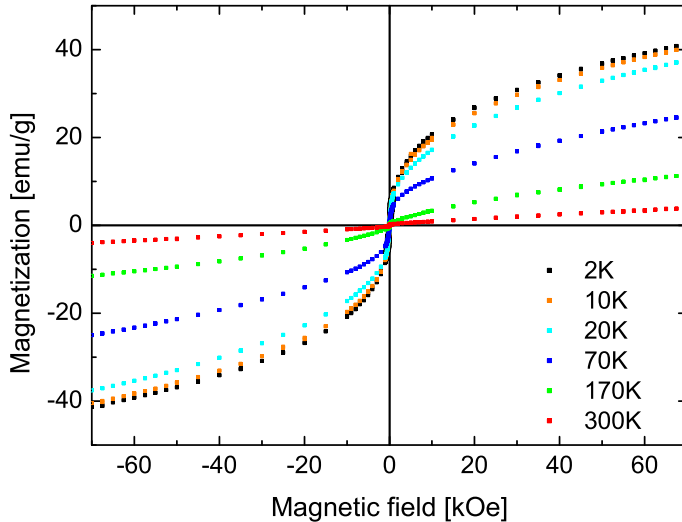


Figure 2: Isothermal magnetization M of $\text{Ni}_2\text{Fe}_{0.5}\text{In}_{0.5}\text{VO}_6$ as a function of an external magnetic field registered at six different temperatures

was observed. On cooling the sample from RT, the EPR amplitude and the linewidth increased and the lineshape became very asymmetrical. An attempt was made to fit the spectrum with the sum of simple Lorentzian or Gaussian lines and the procedure was successful, if at least three Lorentzian lines were used. The temperature

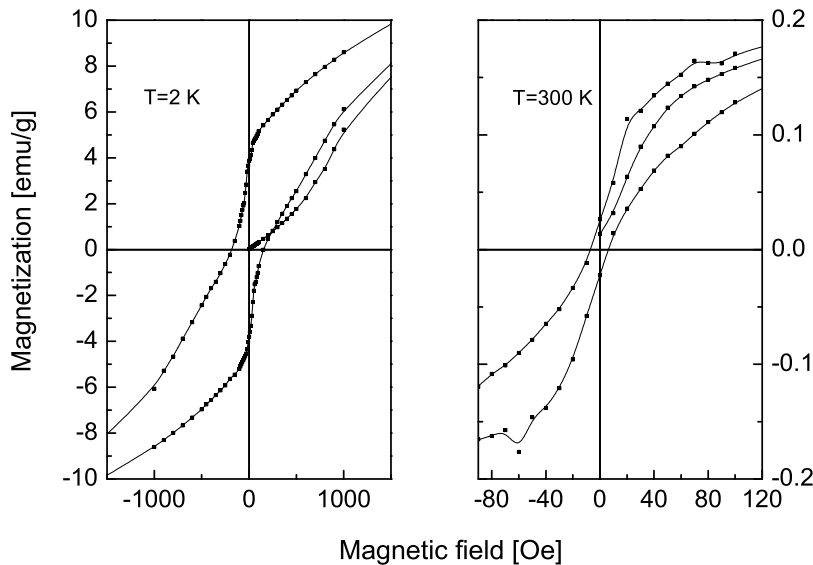


Figure 3: Central part of hysteresis loop registered at 2 K (left panel) and 300 K (right panel)

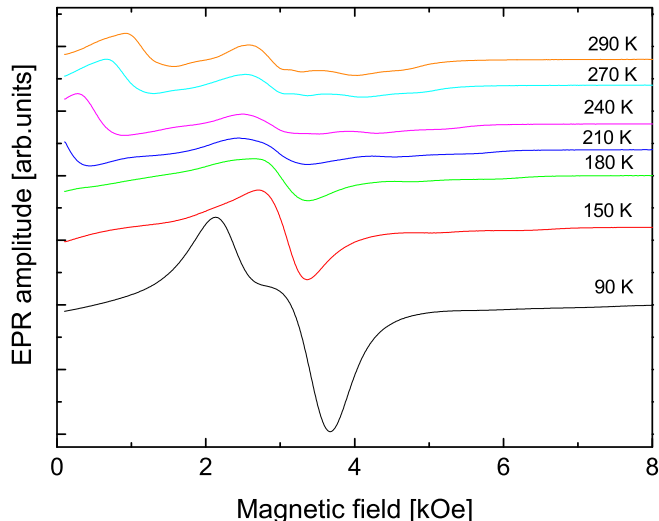


Figure 4: EPR spectra of $\text{Ni}_2\text{Fe}_{0.5}\text{In}_{0.5}\text{VO}_6$ solid solution recorded at several different temperatures

dependence of the resonance field, the linewidth and the integrated intensity of each component line were investigated.

Both types of magnetic measurements (dc magnetization and magnetic resonance) give a consistent picture of the complicated magnetic structure of the $\text{Ni}_2\text{Fe}_{0.5}\text{In}_{0.5}\text{VO}_6$ solid solution. Its magnetic properties are dependent in a large part on Fe^{3+} ions in

a high spin state that are located in layers containing also indium and vanadium ions. Different Fe^{3+} complexes depending on the geometrical arrangements of these ions can be found in these iron layers and involving magnetic V^{3+} and V^{4+} ions are also possible. The magnetization study has revealed at least three different types of magnetic complexes. The low temperature ferromagnetic complex displays its thermal behavior that closely resembles magnetization changes in ferromagnetic magnetic nanoparticles. This suggests that the sizes of magnetic complexes in the $\text{Ni}_2\text{Fe}_{0.5}\text{In}_{0.5}\text{VO}_6$ solid solution might be in a nanometric range.

Magnetic Studies of 0.9(Fe₂O₃)/0.1(ZnO) Nanocomposite: Polymer Matrix Effect

J. Typek¹, K. Wardal¹, G. Zolnierkiewicz¹, N. Guskos¹, D. Siber²,
U. Narkiewicz² and E. Piesowicz³

¹*Institute of Physics, West Pomeranian University of Technology
Al. Piastów 48, 70-311 Szczecin, Poland*

²*Institute of Chemical and Environment Engineering
West Pomeranian University of Technology
Pułaskiego 10, 70-322 Szczecin, Poland*

³*Institute of Material Engineering, West Pomeranian University of Technology
Al. Piastów 19, 70-310 Szczecin, Poland*

Nanocomposites with the general formula $n(\text{Fe}_2\text{O}_3)/(1-n)\text{ZnO}$, where the composition index $0 < n < 1$ have been intensively studied in the recent years. They have been synthesized by two methods: the traditional wet chemical method followed by calcination and the microwave assisted hydrothermal method. Scanning electron microscope images have shown that samples obtained by the latter method are less agglomerated than those obtained by the former. X-ray diffraction and Raman studies have shown that only two phases – ZnO and ZnFe₂O₄- are present in the nanocomposites with the composition index $n \leq 0.70$. In nanocomposites with $n < 0.70$ the presence of yet another phase, $\gamma\text{-Fe}_2\text{O}_3$ (maghemite), has been detected and this phase is dominating in the $n = 0.90$ and $n = 0.95$ samples.

In this report the magnetic properties of 0.9(Fe₂O₃)/0.1(ZnO) nanocomposite synthesized by the traditional wet chemistry method and containing two magnetic phases: $\gamma\text{-Fe}_2\text{O}_3$ and ZnFe₂O₄ (nanocrystallites with the average size of 24 nm) studied by dc magnetization and ferromagnetic resonance (FMR) are presented. The investigated nanocomposites were either the in form of nanopowder or a PTMO-b-PEN polymer matrix dispersed in poly(ethylene naphthalate-block-tetramethylene oxide) at the concentration of 0.1 wt.%. The latter will be designated as the polymer sample.

The FMR spectra of the nanopowder and polymer samples taken at different temperatures in the 4–300 K range are presented in Fig. 1. All the registered spectra could be very well fitted with the sum of two Landau-Lifshitz (LL) lines (Fig. 2). The LL lineshape function is given by the following equation

$$\chi''(H) = \frac{1}{\pi} \frac{H_r^2[(H_r^2 + \Delta_r^2)H^2 + H_r^4]\Delta_H}{[H_r^2(H - H_r)^2 + H^2\Delta_H^2][H_r^2(H + H_r)^2 + H^2\Delta_H^2]} \quad (1)$$

where H_r is the resonance field and Δ_H is the linewidth. The usage of two LL components can be explained by the presence of two different nanoparticles: ZnFe₂O₄ and $\gamma\text{-Fe}_2\text{O}_3$ as evidenced by XRD. It follows from the synthesis reaction that there

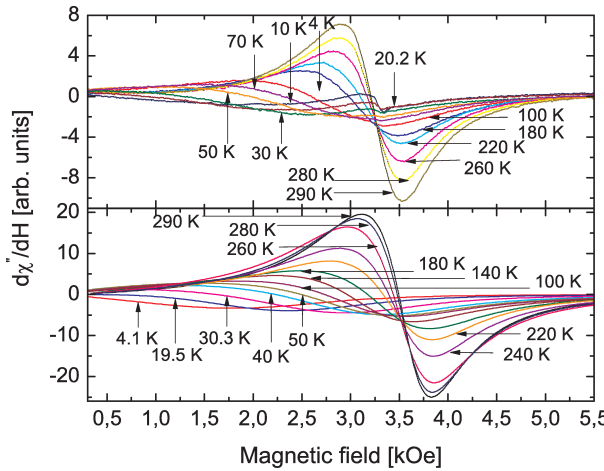


Figure 1: FMR spectra registered at different temperatures: polymer (top panel), nanopowder (bottom panel) samples

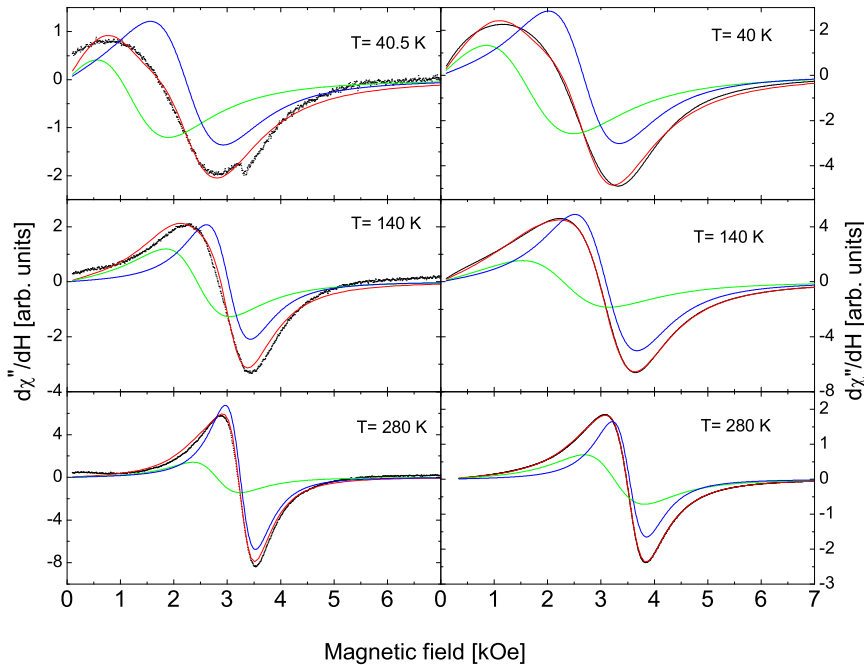


Figure 2: Fitting of observed FMR spectra of nanopowder (left panels) and polymer (right panels) samples with two LL components at three different temperatures

should be 3.62 times more γ - Fe_2O_3 than ZnFe_2O_4 . In Figure 3 the temperature dependence of linewidths and resonance fields of the two components determined from the fittings is presented in the nanopowder and polymer samples. The resonance fields

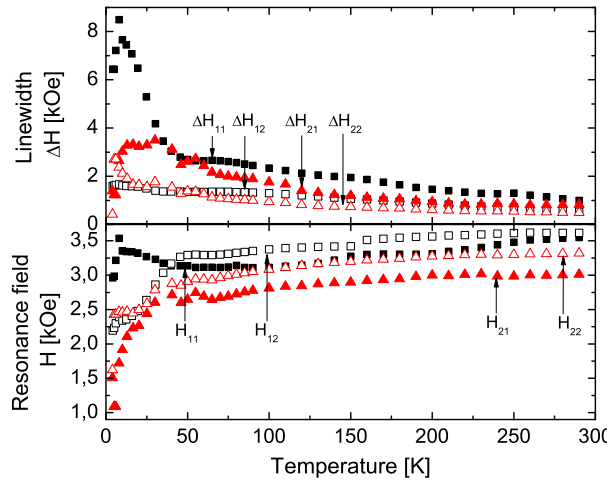


Figure 3: Temperature dependence of linewidths (top panel) and resonance fields (bottom panel) of two components in nanopowder (full and empty black squares) and polymer (full and empty red triangles) samples

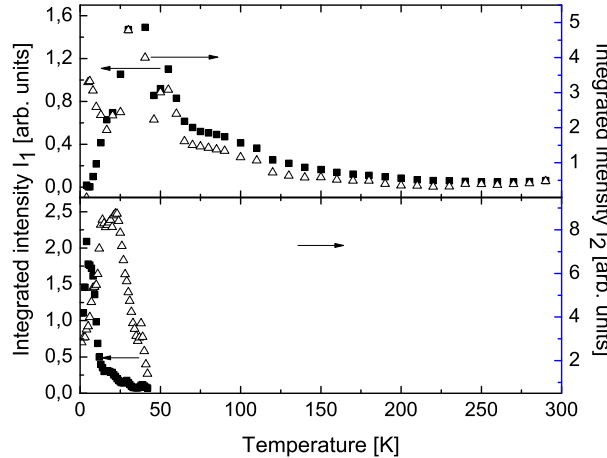


Figure 4: Temperature dependence of integrated intensity of two components in polymer (top panel) and nanopowder (bottom panel) samples. Different left- and right-hand vertical scales are used

and linewidths of components are generally smaller in the polymer sample than in the nanopowder sample what can be explained by lower magnetic anisotropy of nanoparticles. In Figure 4 the temperature dependence of the integrated intensity of the two components in the polymer and nanopowder samples is shown. The ratio of integrated intensity of each component reflects its relative concentration and is consistent with the calculated amount of γ - Fe_2O_3 and ZnFe_2O_4 phases. In the polymer samples both components reach maximum intensity at ~ 40 K, but in nanopowder there is a con-

siderable temperature difference between both maxima. It may indicate the presence of larger aggregates in that sample. Figure 4 shows the temperature dependence of dc susceptibility in the ZFC and FC modes obtained for the nanopowder and polymer samples. The superparamagnetic phase is detected in the high temperature range (depending on the applied magnetic field) Susceptibility in the ZFC mode displays behavior that is typical for nanoparticles with the blocking temperature (~ 50 K in $H = 1$ kOe) which is the same for both sample types. The low temperature behavior of ZF susceptibility in the polymer sample indicates the presence of an additional paramagnetic component.

Peptide-Assisted Synthesis of Metal Oxide Nanostructures

K. Żelechowska¹, P. Golec², J. Karczewska-Golec³, J. Karczewski¹,
A. M. Klonkowski⁴ and G. Wągrzyn³

¹*Department of Solid State Physics, Gdańsk University of Technology
Narutowicza 11/12, 80-233 Gdańsk, Poland*

²*Laboratory of Molecular Biology, Institute of Biochemistry and Biophysics
Polish Academy of Sciences
Wita Stwosza 59, 80-308 Gdańsk, Poland*

³*Department of Molecular Biology, University of Gdańsk
Wita Stwosza 59, 80-308 Gdańsk, Poland*

⁴*Faculty of Chemistry, University of Gdańsk
Wita Stwosza 59, 80-308 Gdańsk, Poland*

Biomineralization, i.e., production of inorganic solids by biological systems has attracted much attention in the field of bionanotechnology. Selected peptides and proteins can facilitate syntheses of inorganic materials at or near room temperature, in aqueous solutions, and at or near neutral pH. Several sequences within natural proteins were identified as mineralizing motifs [1]. Much effort was focused on discovering new inorganic-binding peptides in order to build materials of interest from the bottom-up with nanoscale precision. By adapting biological specificity to materials synthesis and functionality, the generation of structures of controlled composition, size, and shape could be achieved for technologically important applications. We report here peptide directed growth of ZnO and Eu₂O₃ nanostructures. Using the phage display method, derivatives of M13 bacteriophage exposing a ZnO-binding peptide on either pIII or pVIII coat proteins were constructed. Different structures of ZnO were obtained by adjusting the zinc metal ions to the phage ratio. *Inter alia*, nearly spherical nanoparticles of diameters c.a. 50-80 nm were produced. The optical properties of bio-synthesized ZnO nanoparticles were investigated, showing high quality. ZnO NPs synthesized by M13-derived phages form a luminescent material that emits light near the blue part of the visible range ($\lambda_{em} = 400$ nm), with a very low intensity band at 530 nm. Similarly, the M13 bacteriophage exposing Eu₂O₃-binding peptide on pIII was obtained. As a result of phage-assisted synthesis, uniform Eu₂O₃ quantum dots were obtained. The light emission of acquired Eu₂O₃ NPs was demonstrated.

Acknowledgements

This work was supported by the National Science Center (Poland) within Project Grant No. N N302 181439.

References

[1] Smith GP. 1985 *Science* **228** 1315

Magnetic Studies of Three Organometallic Copper Complexes

G. Zolnierkiewicz¹, B. Kolodziej², N. Guskos¹, J. Typek¹, C. Aidinis³
and E. Pilawska¹

¹*Institute of Physics, West Pomeranian University of Technology
Al. Piastów 48, 70-311 Szczecin, Poland*

²*Department of Inorganic and Analytical Chemistry
West Pomeranian University of Technology
Al. Piastów 17, 70-310 Szczecin, Poland*

³*Department of Electronics-Computers-Telecommunications and Control
Faculty of Physics, University of Athens
Panepistimiopolis, 15 784 Zografou, Athens, Greece*

Copper(II) organometallic complexes: Cu(1OXA), Cu(2OXA) and Cu(3OXA) were prepared and studied using the electron spin resonance (ESR) and dc magnetization techniques. Figure 1 presents the chemical structures of the investigated complexes. Figure 2 shows selected EPR spectra of divalent Cu(II) ions in orthorhombic crystal

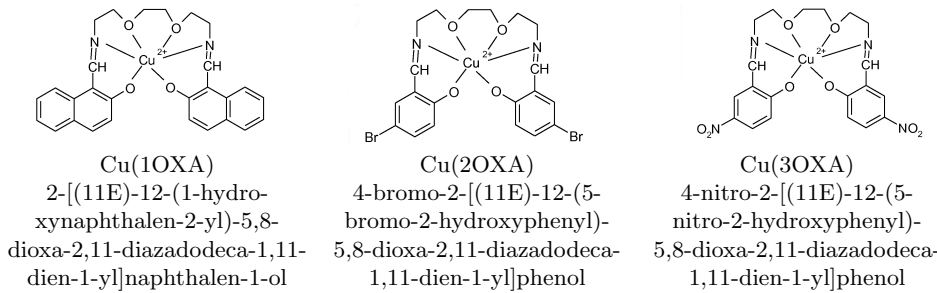


Figure 1: Chemical structure of complexes Cu(1OXA), Cu(2OXA) and Cu(3OXA)

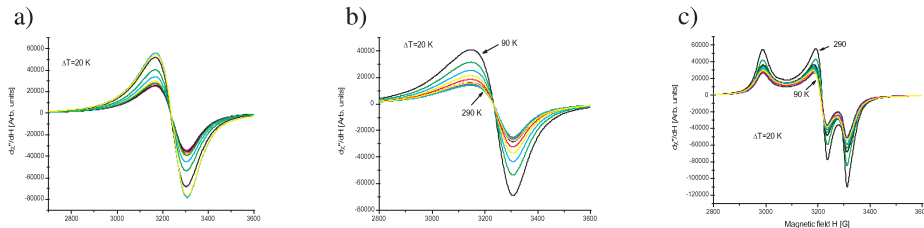


Figure 2: lehead ESR spectra at different temperatures of the complexes: (a) Cu(1OXA), (b) Cu(2OXA) and (c) Cu(3OXA)

fields registered at different temperatures. Numerical deconvolution was carried out for the spectra taken in the 5–295 K temperature range. The powder ESR spectrum was described using three g-factors which strongly depended on the type of the organic matrix. The temperature dependence of ESR integrated intensity showed a Curie–Weiss type of behavior which confirmed the existence of the proposed antiferromagnetic interaction. The temperature dependence of magnetic dc susceptibility suggested the phase transition to the antiferromagnetic phase at 4 K for the Cu(1OXA) complex (Fig. 3a). The magnetic field dependence of the magnetization displayed saturation at low temperature but it was not observed at room temperature (Fig. 3b and c).

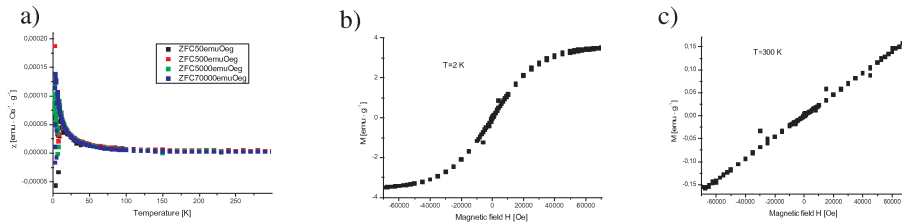


Figure 3: Temperature dependence of magnetic susceptibility (a), field dependence of magnetization at $T = 2$ K (b) and $T = 300$ K (c) for Cu(1OXA) complex

MEDEA'2015

ABSTRACTS

The Phenomenon of Variability in Interior Design in Specific Epochs on the Example of Famous Projects

E. Adam

*Exhibition Design and Scenography Department, Faculty of Visual Arts
Academy of Arts in Szczecin
Szczecin, Poland*

Architectural space design is a process where the architect's idea is embodied in the mutual relation of many factors, such as form, color, texture or light. The final effect appears to be invariable. Observation of the long history of architecture leads to asking the question: Has this invariability been determined by the raw material and the technological progress thereby preventing creation of dynamic, vivid architectural space? Contemporary designs which are subject to fewer and fewer restrictions, moved by sound, light, motion or wind go beyond the patterns established by centuries. Such perception of architecture provides many opportunities for further development, allows its appearance to be determined by not only its creator but the recipient, as well.

The Terms 'Information Society' or 'Digital Society' in the Language of Public International Law

I. Gawłowicz

*Department of Public International and European Law, Faculty of Law and Administration
University of Zielona Góra
Zielona Góra, Poland*

The author examines the terms: 'information society' and 'digital society' in the chosen treaties and in the light of the international custom. The article explores the evolution of the abovementioned terms as well as their meaning and role in public international law and from the perspective of legal culture.

Natural Architectures in Science, Engineering and Medicine

J. N. Grima¹, A. R. Casha² and J. Rybicki³

¹*Faculty of Sciences, University of Malta
Msida, MSD 2080, Malta*

²*Faculty of Medicine and Surgery, University of Malta
Msida, MSD 2080, Malta*

³*Faculty of Applied Physics and Mathematics, Gdańsk University of Technology
Narutowicza 11/12, 80-233 Gdańsk, Poland*

Science, engineering and medicine might seem three very divergent fields. However, encounters between members of these professions often result in discussions and exchanges of how their different worlds are not that dissimilar. Frequently they speak on how the world that surrounds them is so full of inspiration to them in their respective fields. Indeed, one often ignores the obvious and tries to find and invent some complex solutions to their research questions and problems. In the process, sometimes one forgets that, through time, nature has probably already found a way how to solve most problems we will ever encounter, very often in an exceptionally smart manner that we can only but admire and be inspired.

In particular, this article will look at the architectures of the human rib cage and chest and how these are designed for optimal function. It will also look at how the actual chest shape can be modelled using classical pressure vessel theory so as to predict stress concentrations and also the likelihood for certain condition. It will then look at another marvellous natural construct: the shell of turtles and mollusks, and how nature can achieve exceptional mechanical properties in natural hierarchical biomaterials. Finally, it will look at how nature can achieve a highly unusual mechanical property, that of auxeticity, meaning the ability of becoming fatter rather than thinner when stretched, and how this is realised in tendons (including human tendons) and crystals.

Game Engines and New Commercial Market Human-Computer Interfaces on the Way to Web3d

A. Guskos

*Visual Arts Department, Academy of Art in Szczecin
Pl. Orła Białego 2, 70-562 Szczecin, Poland*

Recent emergence and fast development of tools for deployment of dynamical online spatial interactive 3d environments as well as the introduction of a new generation of commercial human-computer interfaces suitable for navigation in these environments are making the idea of Web3d to be closer to come true than ever before. A 3d website development is proposed, based on Unity 3d engine capabilities with a functionality accessible by new human-computer interfaces, such as Oculus Rift, the EMOTIV brain-computer interface or the Razer Hydra game controller.

As It Goes to One Dimension – a Conference Joke

N. Guskos^{1,2}, A. Guskos³ and J. Rybicki⁴

¹*Department of Solid State, Faculty of Physics, University of Athens, Panepistimiopolis, 15784 Zografou, Athens, Greece*

²*Institute of Physics, Western Pomerania University of Technology
Al. Piastów 48, 70-311 Szczecin, Poland*

³*Visual Arts Department, Academy of Art in Szczecin
Pl. Orła Białego 2, 70-562 Szczecin, Poland*

⁴*Department of Technical Physics and Applied Mathematics
Gdansk University of Technology
Narutowicza 11/12, 80-233 Gdańsk, Poland*

Let us take into consideration the road distance between Szczecin and Athens (about 2500 km) and assume that we will cover it by driving a car. We have four coordinates to consider, three of which are spatial dimensions (x, y, z) and the fourth one is time (t). Component z is related to the height and it will increase and decrease during all trip within the range of 1 km. This is a very small fluctuation (0.04%) compared to the overall distance. Let us consider component y which stands for the deviation from the main direction. This inclination will probably not exceed 30 km (12%). The overall fluctuation from the Szczecin–Athens axis during the whole trip will be up to around 1%. In this way we can consider a new set of dimensions: (x, t, f) , where f stands for fluctuation. Keeping that in mind, let us take a look at a conference participant who always reaches his destination. He goes to a tavern and quantizes by a “spiritual intake” in portions of 50 ml (vodka), 100 ml (wine) or 500 ml (beer). A strange phenomenon happens due to the lack of moderation. The coordinate of time (t) almost totally disappears and then, irrespective of the fluctuation value, he finds himself sleeping in his bed. It appears that the only significant coordinate for the conference participant is x .

Abstract for the article for the MEDEA2015 Symposium "Space of Overlapping Interaction"

J. Jurek

*Dean of the Faculty of Interior Design and Stage Design
University of Arts in Poznan
Poznan, Poland*

There are a variety of relations between man and the surrounding space. They are researched by science and envisaged by art. They define human behavior in all situations. In the current development of civilization we realize better and better how numerous and strong ties link us with the environment in the broad sense of the word. With a clarity unknown before, we realize the interrelations, relations and links of people with people, people with the matter, environment and space. The problem of forming zones of overlapping interaction (public facility – city) appears permanently both during the teaching and research program at the Interior Architecture Department at the University of Arts in Poznan, the Academy of Arts in Szczecin and the Faculty of Architecture at the Poznan University of Technology, and in the course of our own design work in the architecture of interior and open spaces of the city, and the downtown in particular.

The adopted basis for research was the forming of zones of overlapping interaction in the urban space which is significantly affected by public buildings and the related problems of organizing the space for the needs of emotional reception and participation in culture.

Types of public buildings were analyzed in terms of their effect in the space of overlapping interaction, and the occurrence of the issue formulated in the title was analyzed as a conscious act of creation on the basis of study and diploma designs, those existing contemporarily and those developed at Polish universities of art.

Parallel Techno Creation in Audiovisual Art

I. Kuriata

*Faculty of Visual Arts, Szczecin Academy of Arts
Pl. Orła Białego 2, 70-562 Szczecin, Poland*

An important factor in the development of electronic music is the technological progress. Continuous evolution of analogue and then digital methods of developing the sound has always had a significant impact on the experimental nature of this field of art. Thus, the emergence of new instruments, or generally speaking, all implements of musical production, has repeatedly contributed to the development of new styles and ways of artistic expression.

The digital age has provided musicians with the possibility of self-recording and production of their accomplishments through a DAW (digital audio workstation). In this way, the artist has become also the producer of his recordings which has allowed him to have unlimited control over the produced material, and eventually full creative independence.

Subsequently, the parallel progress of digital video technology has provided the artist with an opportunity of working simultaneously with sound and image. Importantly enough, both factors are treated here on equal terms – the image is not at the service of sound as is the case with music video clips, and the music does not play the role of the background as is the case with movie productions.

The software allows the visual layer to respond immediately in real time as certain audio frequencies are assigned to selected parameters, it responds to the midi controller movements or becomes a surgical tool of a well thought-out project. Owing to this the visual part has acquired a new meaning or taken an abstract form, appropriate for the non-figurative property of sound.

As it turns out the digital technology enables the artist to preserve individuality through full control over all the project stages. It can also become a co-creator performing with the human being in a creative duo or allow the artist to create a work of art living as if its own life.

Empathy in Designing as Manifestation of a New Attitude of Contemporary Designers

J. Machnicka

*Faculty of Visual Arts, Academy of Arts in Szczecin
Szczecin, Poland*

The present days do not put us in a cheerful mood. More and more clearly we can see the negative changes occurring in the surrounding world. Thanks to the media, we can see it in a broader global perspective. Environmental pollution which affects the climate changes that have been noticeable for many years, civilization diseases, unreasonable excessive consumerism, waste of food or the growing gap between the rich and the poor – these are only some out of the many examples of the phenomena that have appeared in the contemporary world as an answer to the general egoism among people. However, for some time, it has been possible to observe changes in our behavior, in thinking which is no longer focused only on ourselves, but goes beyond the fulfillment of our own needs, without looking at the effects of such actions. There are more and more people who wish, on their own initiative or organizing themselves in groups, to implement changes so as to, for example, save the environment. Occasionally, some people undertake daring actions showing that it is possible to live differently, e.g. the Jonsons, a family of four from California that produces only one jar of garbage a year, following the zero waste philosophy, whereby they prove that anything is possible, the only thing to do is to change the stereotypical way of thinking and one's lifestyle. Also large companies, such as Ikea try to adapt their products to the requirements of the customer who is thinking about the future of our planet. Consumers slowly begin to feel the need to do something useful for the environment. And most importantly, they understand that they should start with themselves. Also designers are changing their way of thinking about the design as their work is primarily an intellectual activity. We are brought up in the culture of image, and everyone knows that its power is greater than the power of a word or text. Image affects our life, communication, understanding of the surrounding reality. With it, designers can affect people, encourage them to change, to feel empathy. Also among students a different approach to their works created in art schools can be seen. At the defense of recent MA projects at the Department of Design Graphics of the Faculty of Visual Arts it was possible several times to hear the words of students defending their projects saying the they do not want to design for their own pleasure but that they wish to do something for others who are often weaker and in need. It was empathy that motivated them to create and activated to act.

Commemoration – an Archetype of Future

K. Radecka

*Faculty of Visual Arts, Academy of Arts in Szczecin
Pl. Orła Białego 2, 70-562 Szczecin, Poland*

The need to commemorate people and events to the memory of community or our own past dates back to the beginnings of mankind, the resultant artifacts create the identity of heirs of their creators. Commemoration may be expressed as an image, sound, written word, real or virtual structure. In this work I wish to focus on monument forms as works of art most distinctly addressed to the social awareness and most permanently manifesting themselves in the public space.

The material objects of memory were posthumous signs of human existence related to the place of burial. They manifested themselves in various graveyard forms, from modest symbols to monumental buildings. The sepulchral art was developing along with the development of necropolises. The memory of events was commemorated as early as in the ancient times emphasizing their significance by formal references to the architecture – construction elements important for the structure. Their size (scale) reflected the momentousness of the immortalized history, and the main emotion evoked was admiration.

The dramatic events of the 20th century had a significant impact on the visual appearance of monumental commemoration leading it back to the rudiments of culture. Reflection of unimaginable things, the enormity of cruelty, the immenseness of evil forced commemorative creators to use emotionally moving solutions realized by symbolic architectural structures.

The formal means of artistic expression in memorial sites such as Auschwitz, Treblinka, Belzec or Sobibor should be the silence. Silence and emptiness experienced sensually and mentally can tell more about past events than any realistic forms. Perhaps, the phenomenon of such places should be addressed not by the language of the humanities but the language of quantum physics as these are “phenomena” which are not subject to “direct perception”. It should be considered whether, using the state-of-the-art technology, the method of commemoration could be changed to avoid the necessity of deforming the naturally or historically formed space and communicate the required information and emotions without resorting to grotesque dioramas and hardly credible reconstructions.

A Diary of a Visual Artist – Hommage‘á Roman Opalka

G. Radecki

*The Inter-Faculty Institute of Art Sciences, Academy of Fine Arts in Gdańsk
Gdansk, Poland*

In the abundance of achievements and advantages brought by the IT revolution we can turn to our advantage the renaissance of communication between people, particularly through social forums or daily entries made in a kind of a diary which is nowadays called a blog. However, these modern forms resembling a diary, published online, enabling authors to instantly share their experiences or thoughts, as well as immediately respond to the comments of Web users bring associations rather with a conversation and are fairly remote from records called a memoir from the point of view of the diary tradition. Originally, these traditional diaries were to serve only the author and his or her close ones, and they were not addressed to a wider public, at the most, their recipients could be readers from some distant future, as the regular entries were conceived to be a type of a personal memoir without any self-censorship.

An interesting manifestation related, in my opinion, to the original genre of a journal – in the literary form known from books, is a certain activity of visual artists the origin of which is also related to emphasizing the problem of human perception of the passing time. It consists in undertaking certain standardized activities, repeated consistently and regularly over some longer period of time with the effect in the form of visual artifacts. The most renown artist performing activities of this type and also pursuing this program most fully and with unrelenting consistency was Roman Opalka. His most famous work is the series *Opalka 1965/1 – ∞*. The artist put series of digits on canvas in white paint; initially he did it on black canvas, then changed it to grey to gradually lighten up the background as of 1972. In addition to that he pronounced each digit recording it on a tape-recorder, and added his current photograph to the finished painting.

Impressed by the extraordinary creativity of this artist, I have decided to utilize the potential offered by the state-of-the-art digital technology for the purposes of my own activities having the nature of a chronicle illustrating the experience of the passing days. The program which I have taken up, the assumptions and effects of which I share in my presentation, fits in with the underling idea of the symposium – the venerable literary form of a diary meeting halfway the contemporary visual medium realized in the form of digital graphics. Regularly created images, unified in terms of form, when juxtaposed, perfectly illustrate the variability and subjective nature of experiencing subsequent days, months and years.

Self-Similarity in Architecture

A. Rybicka¹, J. S. Rybicki², J. N. Grima³ and J. Rybicki^{1,4}

¹ *Department of Solid State Physics, Faculty of Applied Physics and Mathematics
Gdansk University of Technology
Narutowicza 11/12, 80-233 Gdansk, Poland*

² *Wyspianskiego 25/9, 80-434 Gdansk, Poland*

³ *Metamaterials Unit, Faculty of Science, University of Malta
Msida, MSD 2080, Malta*

⁴ *TASK Computer Centre, Gdansk University of Technology
Narutowicza 11/12, 80-233 Gdansk, Poland*

Fractals are systems which exhibit a repeating pattern that re-displays itself at every scale. Benoit Mandelbrot has given numerous examples of the occurrence of fractals in various places in nature. A fractal object is self-similar which means that when all the dimensions of the structure are modified by the same scaling factor, an object that looks similarly as the original (not scaled) object is obtained. 'Looks similarly' means that the scaled object can be translated and/or rotated, can be smaller or larger, but its shape remains similar: the relative proportions of the sides and internal angles of the shape remain unchanged. We usually appreciate self-similarity in designed objects. One can easily show that artists and architects have exploited fractal structures for centuries.

In this paper a number of examples of self-similar designs – intuitive and conscious – in architecture in various epochs (from the Middle Ages to the present times) and in various civilizations (Oriental and Western) are presented. Hindu Mandala and Dante's universe will be discussed as examples of self-similar heaven architecture.

Architecture vs. Mathematics in Ancient Egypt

A. Rybicka¹, J. S. Rybicki², J. N. Grima³ and J. Rybicki^{1,4}

¹ *Department of Solid State Physics, Faculty of Applied Physics and Mathematics
Gdansk University of Technology
Narutowicza 11/12, 80-233 Gdansk, Poland*

² *Wyspianskiego 25/9, 80-434 Gdansk, Poland*

³ *Metamaterials Unit, Faculty of Science, University of Malta
Msida, MSD 2080, Malta*

⁴ *TASK Computer Centre, Gdansk University of Technology
Narutowicza 11/12, 80-233 Gdansk, Poland*

Mathematics has always played an important role in architecture. However, nowadays it is not easy to understand exactly the relationship between mathematics and architecture in ancient civilizations. A contemporary researcher can be easily deceived by being accustomed to the contemporary relationship between architecture and mathematics or computer science, and it may be hard for him to step into the shoes of the ancient architect as it is not easy to forget about the progress in mathematics made since then. Indeed, very many earlier and contemporary works are tainted by anachronism. Another difficulty, this time of a technical nature, is the unverified reliability of ancient drawings and sketches, as well as the uncertainty as to the actual measure of the units used in antiquity.

Current knowledge on ancient Egyptian mathematics will be reviewed in the lecture. Also discussed are the theories suggested in the past to explain the proportions in the ancient Egyptian art, focusing on methodological errors, still influencing negatively our understanding of the Egyptian art. The second part of the lecture will be devoted to a detailed analysis of the archaeological evidence on the design and construction processes, giving a realistic image of how mathematics was used by ancient Egyptian architects and workmen.

INDEX OF AUTHORS

Adam, E., 79
Adamski, P., 33
Aidinis, C., 34, 75
Arabczyk, W., 16, 33, 42
Attard, D., 11, 15, 19, 27, 29, 43
Azzopardi, K. M., 27
Bennaceur, R., 61
Berczynski, P., 32
Bilewicz, R., 60
Blonska-Tabero, A., 34
Bobrowska, M., 62, 66
Bochentyn, B., 12, 14
Brincat, J.-P., 27
Calleja, C., 11
Caruana-Gauci, R., 19, 29
Casha, A. R., 15, 81
Cauchi, R., 11, 26
Chmielewski, R., 16
Diamantopoulou, A., 18, 32, 36
Diez, J. V. Munoz, 31
Dudek, K. K., 15, 19, 29
Dziedzic, J., 20, 22, 24
Filipek, E., 62, 66
Formosa, J. P., 26
Gambin, D., 27, 28
Gatt, R., 15, 27, 28, 29, 43
Gauci, M., 15
Gawłowicz, I., 80
Glenis, S., 18, 32, 36
Golec, P., 74
Grima, J. N., 11, 15, 19, 26, 27, 28, 29, 43, 81, 89, 90
Grinberg, M., 30, 49
Gulkowski, S., 31
Guskos, A., 32, 33, 36, 82, 83
Guskos, N., 18, 32, 33, 34, 36, 49, 56, 70, 75, 83
Hełminiak, A., 42
Jaziri, S., 61
Jenczyk, J., 38
Jurek, J., 84
Kapica-Kozar, J., 36, 44
Karczewska-Golec, J., 74
Karczewski, J., 12, 60, 74
Kempinski, M., 38, 39
Kempinski, W., 39
Kindrat, I. I., 49
Klonkowski, A. M., 74
Kolodziej, B., 75
Kondratowicz, I., 40, 41
Konicki, W., 42
Kukliński, B., 49
Kulyk, Y. O., 49
Kuriata, I., 85
Kusiak-Nejman, E., 36, 44

Kusz, B., 12, 14, 60
Likodimos, V., 18
Liudkevych, U., 46
Machnicka, J., 86
Mahlik, S., 49
Majdecka, D., 60
Manch , A., 15
Markowski, D., 39
Michalkiewicz, B., 44
Miruszewski, T., 12
Mizzi, L., 43
Morawski, A. W., 36, 44
Mosnacek, J., 56
Moszy ski, D., 33
Mudry, S., 46, 47
Mudry, S. I., 49
Narkiewicz, U., 44, 70
Narojczyk, J. W., 48
Paczesna, A., 62, 66
Padlyak, B. V., 49
Papadopoulos, G. J., 52
Paszkiewicz, S., 53, 56
Pawelec, I., 53, 56
Petridis, D., 32
Piesowicz, E., 70
Pig owski, P. M., 48
Pilarska, M., 34
Pilawka, R., 53
Pilawska, E., 36, 75
Pir g, E., 44
Plechystyi, V., 55
Pozniak, A. A., 43
Radecka, K., 87
Radecki, G., 88
Ros aniec, Z., 53
Rybicka, A., 89, 90
Rybicki, J., 24, 81, 83, 89, 90
Rybicki, J. S., 89, 90
Sadowski, W., 41
Shtablavyi, I., 46, 47, 55
Sibera, D., 70
Skylaris, C.-K., 20, 22
Sliwinska-Bartkowiak, M., 38
Spitalsky, Z., 56
Szreder, N., 14
Szymczyk, A., 53, 56
Trawi ski, B., 60
Tretiakov, K. V., 48
Triki, M., 61
Typek, J., 32, 33, 34, 36, 56,
62, 66, 70, 75
Wanag, A., 36, 44
Wardal, K., 70
Warych, A., 14
W grzyn, G., 74
Winczewski, S., 24
Wojciechowski, K. W., 19, 29, 43, 48
Wolak, W., 15
Wood, M. V., 27
Wr bel, R. J., 44
Zolnierkiewicz, G., 18, 33, 34, 36, 49,
56, 62, 66, 70, 75
 elechowska, K., 40, 41, 60, 74